



**Trip Report for**  
**“ACS 233<sup>rd</sup> National Meeting and Exposition”**  
**Chicago, Illinois**  
**March 25 – 29, 2007**

**Feryan Ahmed, Ph.D.; Van-Duc Le, Ph.D.;**  
**Joe Raker, Ph.D.; Hong-Jun Wang, Ph.D.**

---

**Abstract:** *The 233<sup>rd</sup> ACS National Meeting and Exposition was held in Chicago, IL from March 25 – 29, 2007. This report highlights selected material presented at the conference.*

---

**“Discovery of potent, selective and orally bioavailable CCR5 antagonists”**

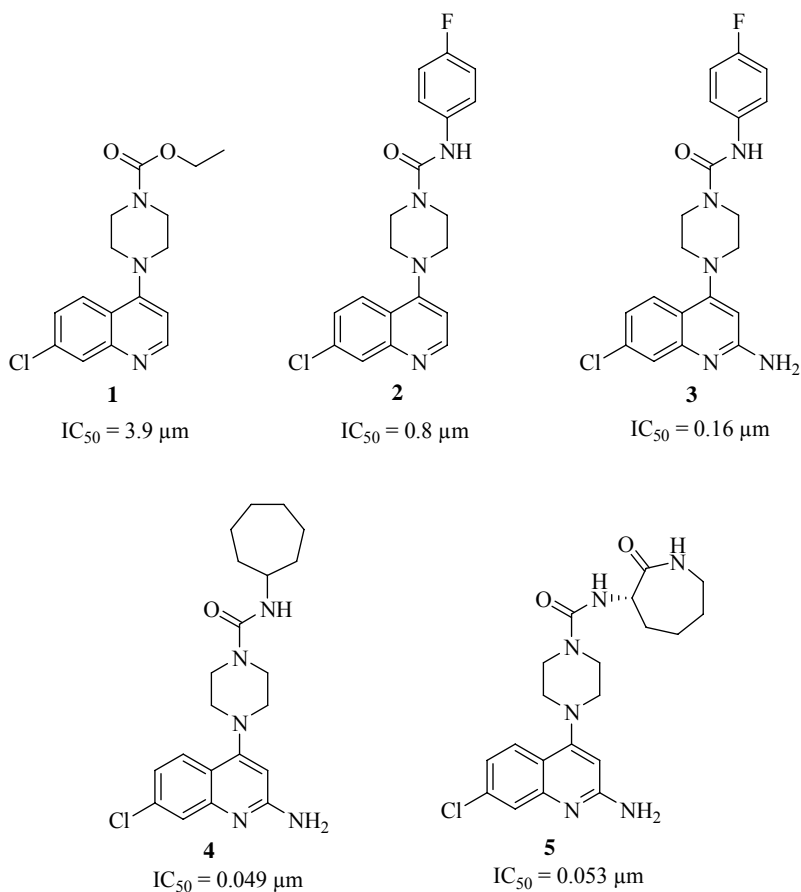
*Robert G. Wei, Shou-Fu Lu, Binglong Chen, Kieu Chu, Dave Davey, Laura Dunning, Elena Ho, Stefan Jaroch, Monica Kochanny, Wheeseong Lee, Xiongdong Lian, Zhiyun Ma, James Onuffer, Gary Phillips, Babu Subramanyam, Jih-Lie Tseng, Janette Walters, Ming Wei, and Bin Ye, Berlex Biosciences, 2600 Hilltop Drive, Richmond, CA 94806*

The CC chemokine receptor-5 (CCR5) acts as one of the co-receptors for the entry of macrophage-tropic strains of HIV-1 into cells and has been a focus of drug discovery efforts. CCR5 has also been implicated in diseases of the brain, including multiple sclerosis (MS), where

it has been detected on activated myeloid microglial cells and infiltrating T cells in lesions. CCR5 antagonists are useful in suppressing chronic inflammatory symptoms of these diseases.

Using high throughput screening and automated chemical synthesis, researchers at Berlex identified quinoline containing compound **1** and **2** as CCR5 antagonists (Figure 1). Optimization of the quinoline ring led to the discovery of compound **3** with improved potency ( $IC_{50} = 160$  nM). Replacement of the 4-fluorophenyl group with cyclic rings led to the new lead compound **5**. Among the cycloalkyl groups, cycloheptyl offered the best potency, but was highly metabolized. The L-caprolactam provided similar potency with improved metabolic stability, but poor PK.

**Figure 1**



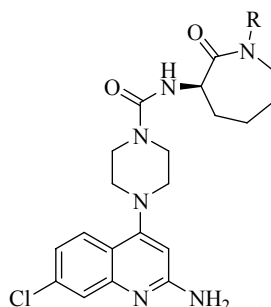
Further studies were conducted toward different *N*-substituted L-caprolactams, and the results are summarized as follow:

1. *N*-Alkyl groups gave good potency, but poor PK, and compounds were metabolized to give **5**.
2. Introduction of *N*-acetyl group improved the PK, but compound decomposed to give **5**.
3. *N*-Methylsulfonyl and phenylsulfonyl groups resulted in poor PK.
4. *N*-Alkoxy carbonyl and phenoxy carbonyl groups were good for potency, and compound **6** offered good PK.

5. *N*-Alkylamido groups led to the discovery of potent, selective and orally bioavailable CCR5 antagonists **7** and **8**.

The SAR for the L-caprolactams is shown below (Figure 2).

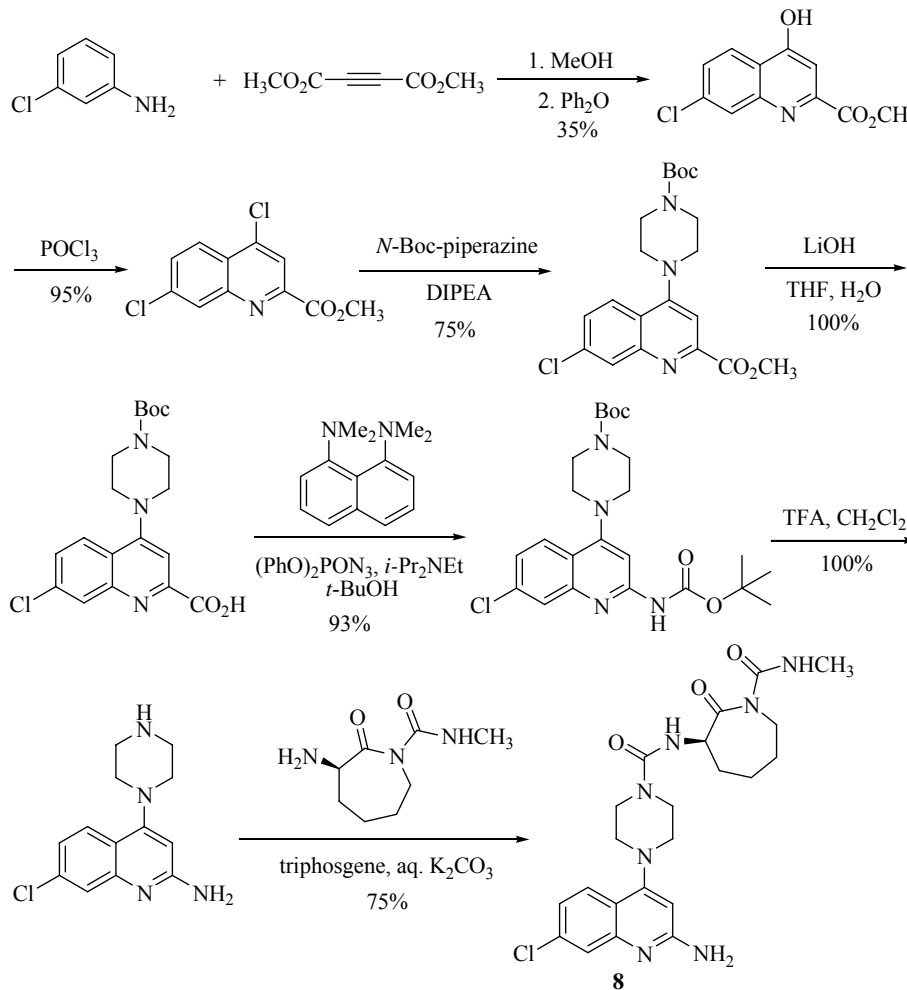
**Figure 2**



R =	CO <sub>2</sub> CH <sub>3</sub>	CONHEt	CONHCH <sub>3</sub>
	<b>6</b>	<b>7</b>	<b>8</b>
	IC <sub>50</sub> = 22 nm (binding)	IC <sub>50</sub> = 21 nm (binding)	IC <sub>50</sub> = 22 nm (binding)
	IC <sub>50</sub> = 24 nm (Ca <sup>2+</sup> , flux)	IC <sub>50</sub> = 23 nm (Ca <sup>2+</sup> , flux)	IC <sub>50</sub> = 15 nm (Ca <sup>2+</sup> , flux)
	t <sub>1/2</sub> = 1.2 h (rat, PO)	t <sub>1/2</sub> = 1 h (rat, PO)	t <sub>1/2</sub> = 1.4 h (rat, PO)
	F% = 36% (rat)	F% = 78% (rat)	F% = 73% (rat)

Compound **8** was synthesized on a 25 g scale in 8 steps, with 17.4% overall yield, >99% purity and 99% ee being achieved (Scheme 1).

### Scheme 1



In conclusion compound **8** shows:

1. High potency as CCR5 antagonist:  $IC_{50} = 15 \text{ nm}$  ( $Ca^{2+}$ , flux)
2. Good selectivity
3. Good oral bioavailability:  $F\%$  (rat) = 73%;  $t_{1/2} = 1.4 \text{ h}$  (rat, PO) and  $F\%$  (dog) = 91%;  $t_{1/2} = 5.0 \text{ h}$  (dog, PO)
4. Low inhibition of CYP<sub>450</sub> enzymes

#### “Tetrahydrocarbazole amides as potential agents for treatment of papillomavirus infection”

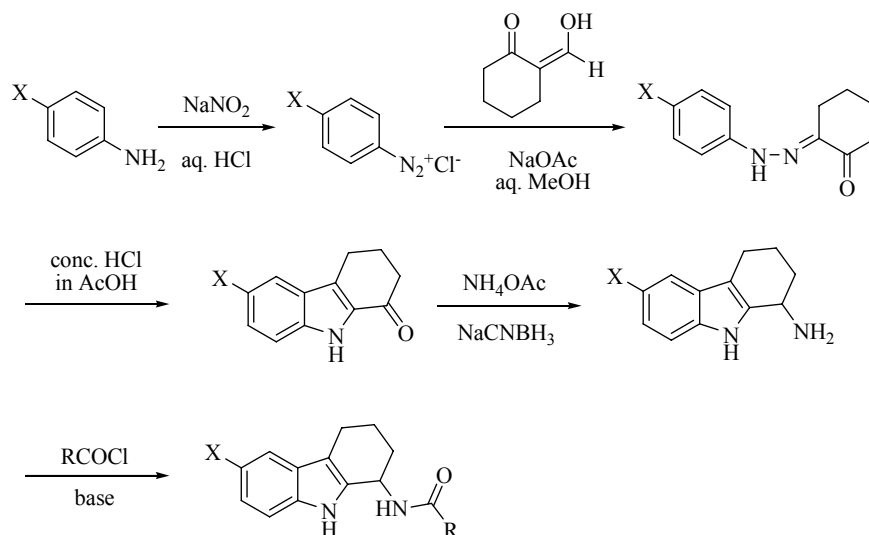
*Kristjan Gudmundsson<sup>1</sup>, Sharon Boggs<sup>1</sup>, David Haigh<sup>1</sup>, Brian Johns<sup>1</sup>, Leah Richardson<sup>1</sup>, Paul Sebahar<sup>1</sup>, Jason Weatherhead<sup>1</sup>, Kevin Brown<sup>2</sup>, Robert Harvey<sup>2</sup>, Phiroze Sethna<sup>2</sup>, Qin Zhang<sup>2</sup>, Pamela Golden<sup>3</sup> and Shiping Xie<sup>4</sup>*

*Department of Medicinal Chemistry<sup>1</sup>, Department of Oncogenic and Emerging Viruses<sup>2</sup>, Drug Metabolism and Pharmacokinetics<sup>3</sup>, and Chemical Development<sup>4</sup>, GlaxoSmithKline, Five Moore Drive, Research Triangle Park, NC 27709,*

Human papillomaviruses (HPVs) are small DNA viruses that infect the genital mucosa, and are considered the most common sexually transmitted disease throughout the world. There are over

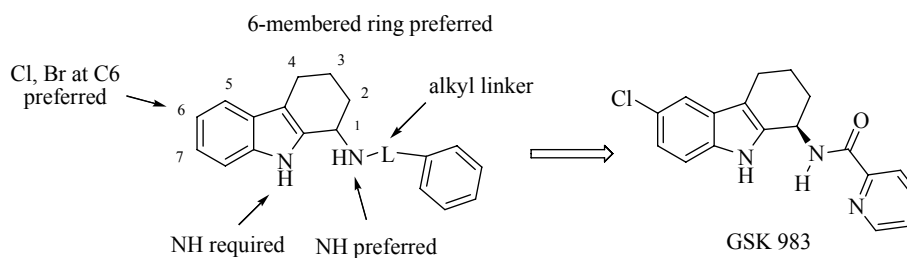
5.5 million new cases of HPV in the US each year. Currently available treatments for HPV infection do not target the virus and are invasive, involving surgical removal or chemical destruction of the infected tissues. Researchers at GlaxoSmithKline have discovered molecules that target high risk HPVs for the treatment of cervical dysplasia (Scheme 1).

**Scheme 1**



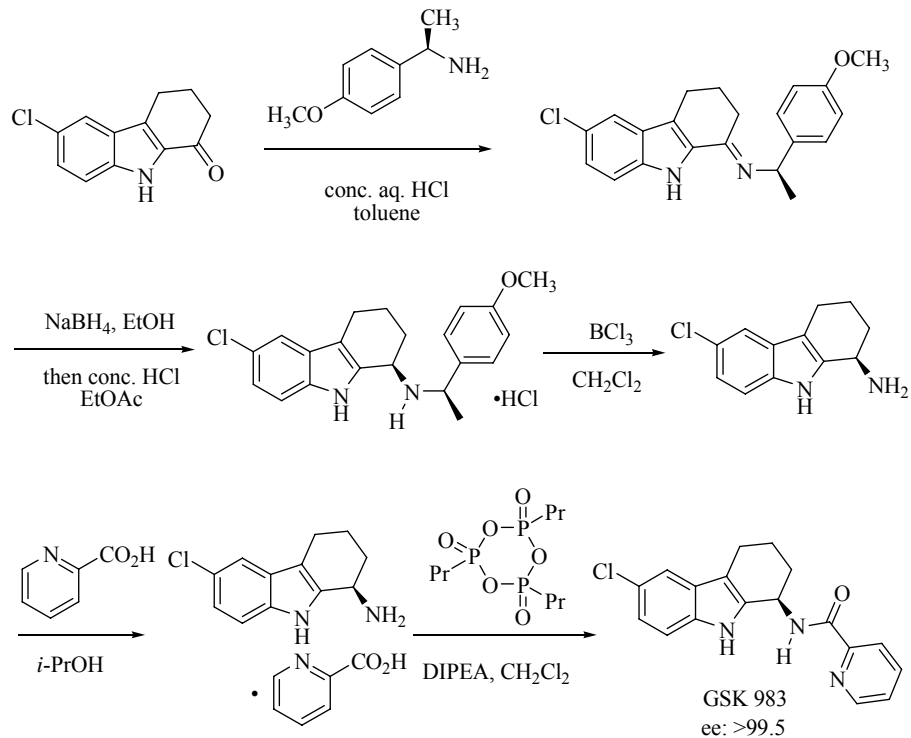
The tetrahydrocarbazole scaffold was identified from high throughput screening. Initial SAR (Figure 1) revealed that benzamides gave optimal anti-HPV potency and adding substituents on the benzamide further improved potency.

**Figure 1**



Further studies indicated that the R-isomers were very potent, while the S-isomers were inactive. A chiral synthetic route (Scheme 2) was developed to scale up kilogram quantities with high enantiomeric purity.

## Scheme 2



In conclusion GSK 983 shows:

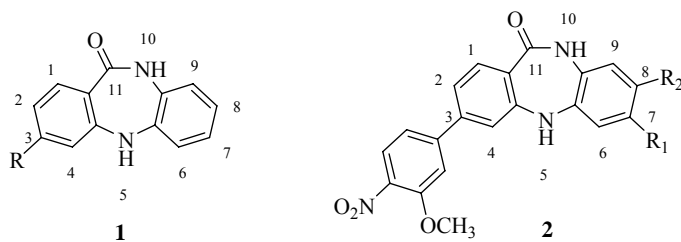
- 1) Potent anti-HPV activity in the W-12 assay system
- 2) Similar activity against HPV-16 and HPV-31
- 3) Potent activity in raft tissue culture systems
- 4) Good separation between antiviral activity and toxicity
- 5) Good pharmacokinetic profile in rats, dogs and monkeys
- 6) No cytochrome P450 inhibition

---

**“Investigation of novel 7,8-disubstituted-5,10-dihydro-dibenzo[b,e][1,4]diazepin-11-ones as potent and selective Chk-1 inhibitors”**, Lisa A. Hasvold, Le Wang, Gerard M. Sullivan, Magdalena Przytulinska, Laura Hexamer, Zhan Xiao, Zehan Chen, Wen-Zhen Gu, Philip J. Merta, John Xue, Peter Kovar, Haiying Zhang, Jennifer Bouska, Chang Park, Thomas J. Sowin, Saul H. Rosenberg, and Nan-Horng Lin  
*Cancer Research, Abbott Laboratories, Abbott Park, IL 60064-6101.*

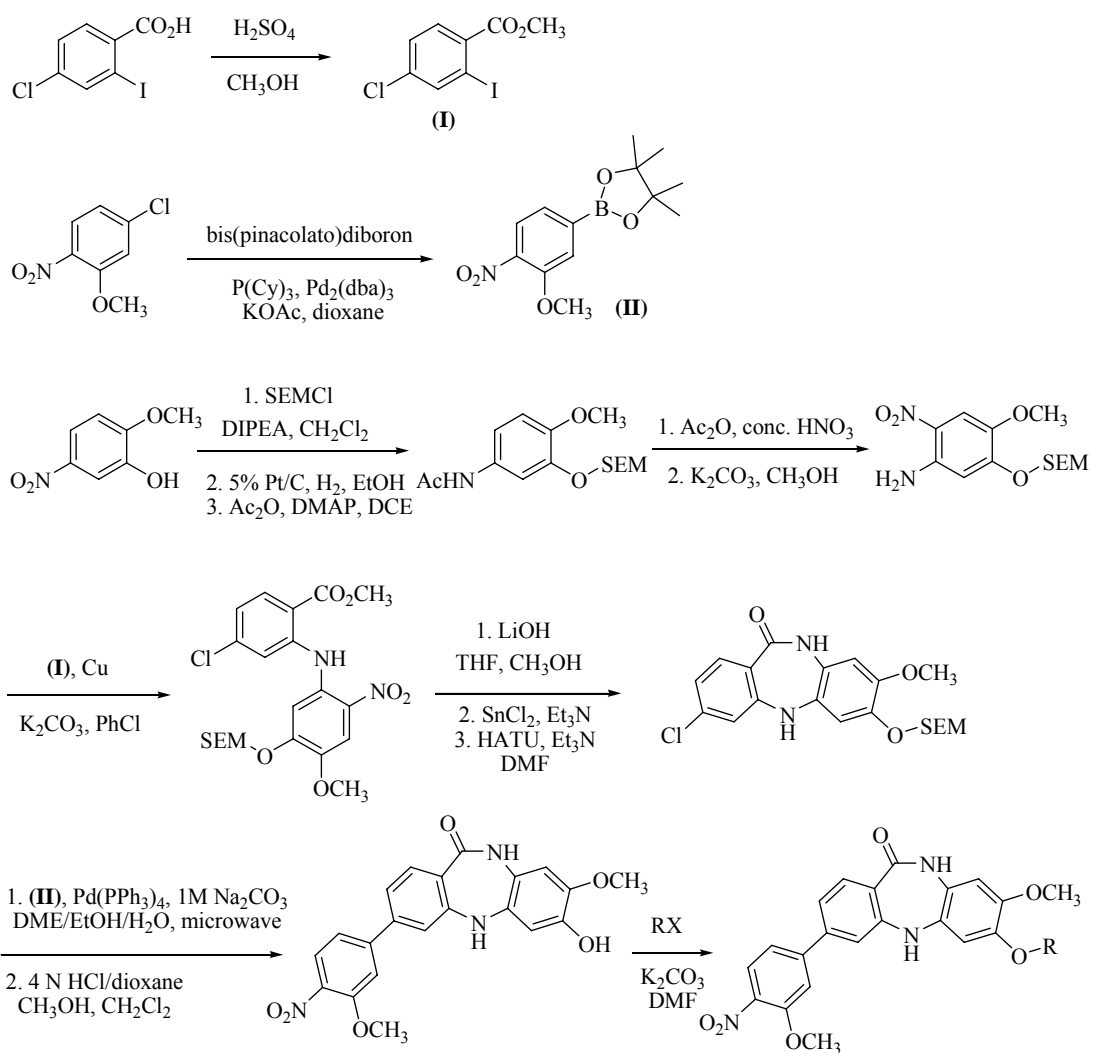
Checkpoint kinase 1 (Chk-1) functions as a regulator by arresting DNA damaged cells at the G2/M checkpoint to prevent cells from entering mitosis, so that the DNA repair mechanism can be carried out. It is thought that inhibition of Chk-1 will lead to abrogation of the G2/M checkpoint, thus allowing DNA-damaged cells to enter mitosis, ultimately resulting in cell death. Researchers at Abbott have identified a series of 5,10-dihydrodibenzo[b,e][1,4]diazepin-11-one compounds **1** as potent and selective Chk-1 inhibitors (Figure 1). In an attempt to improve the biological profile of the benzodiazepinone compounds, a variety of 7,8-disubstituted-5,10-dihydro-dibenzo[b,e][1,4]diazepin-11-one compounds **2** were prepared in which the 3-position of the core was held constant as the 3-methoxy-4-nitrophenyl moiety.

**Figure 1**

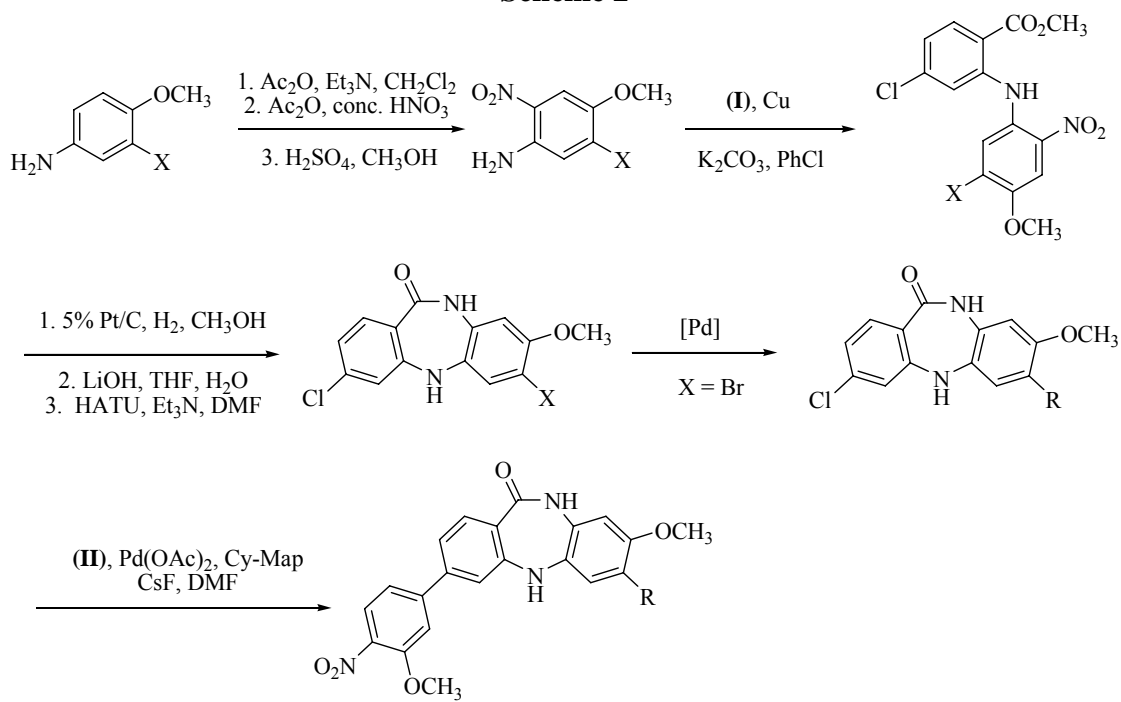


Shown below in Schemes 1-4 is a summary of the synthetic efforts.

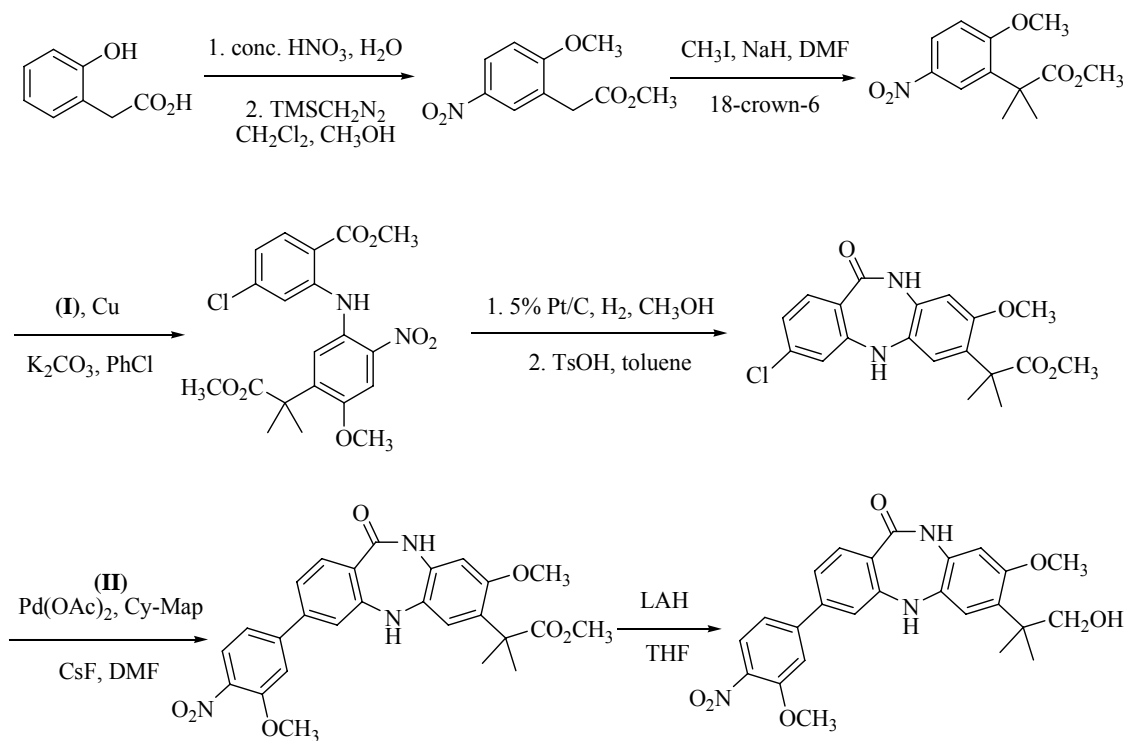
**Scheme 1**



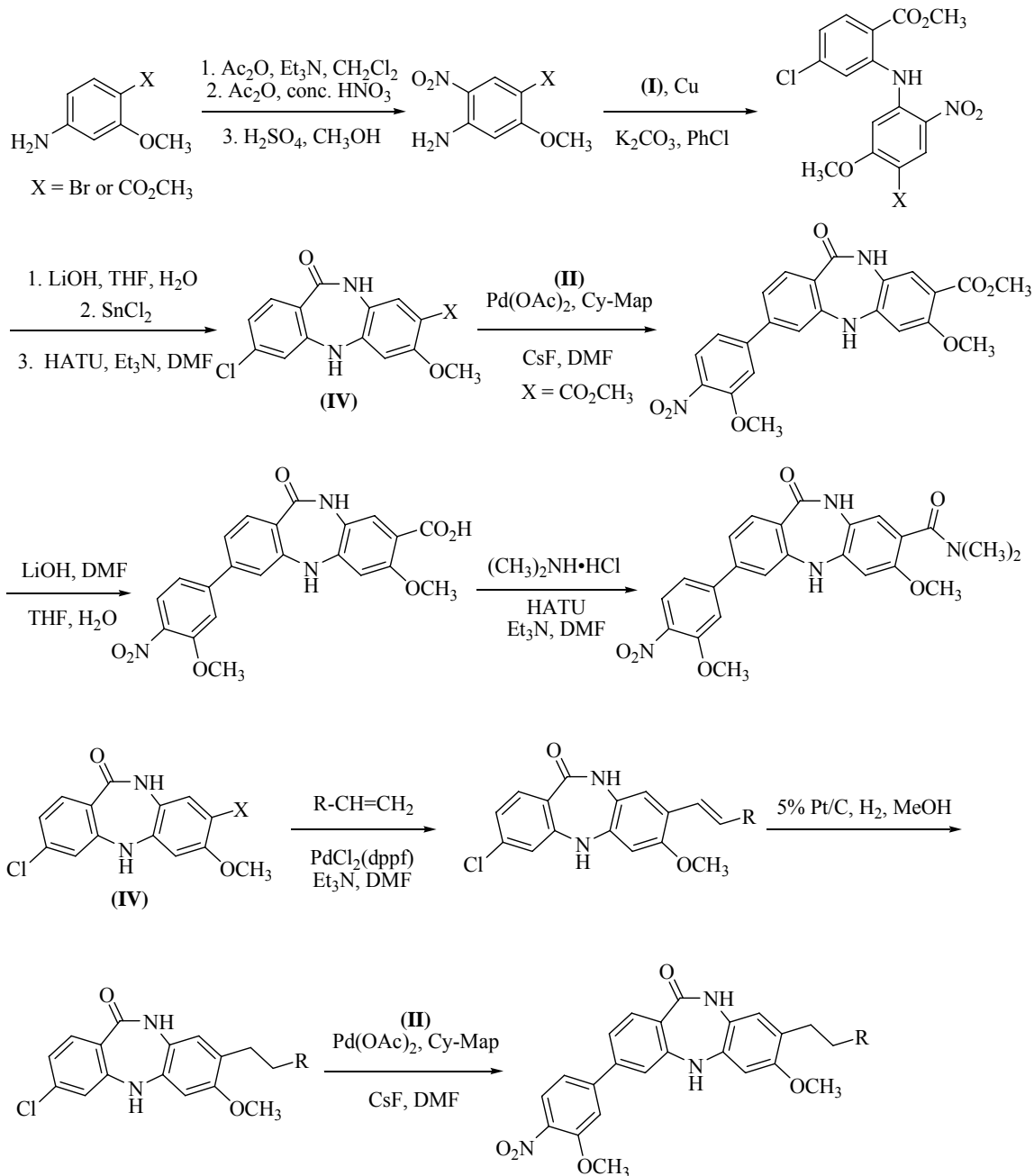
### Scheme 2



### Scheme 3

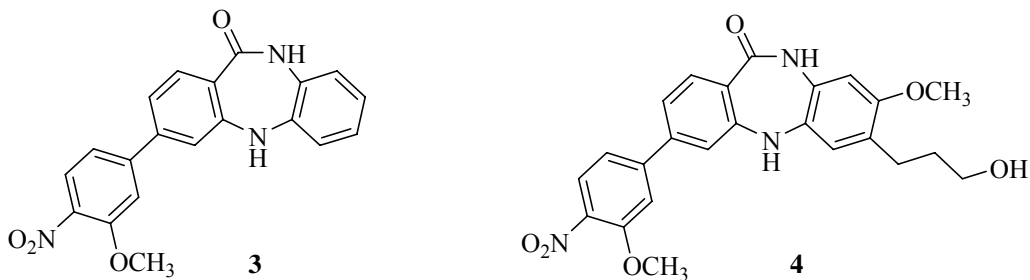


### Scheme 4



A variety of 7,8-disubstituted 5,10-dihydrodibenzo[b,e][1,4]diazepin-11-one compounds were prepared in an attempt to improve the biological profile of compound **3** (Figure 2), which possessed good enzymatic activity ( $\text{IC}_{50} = 10 \text{ nm}$ ), but was not active in cells (MTS assay combination  $\text{EC}_{50} = 33.8 \text{ }\mu\text{M}$ ). Several compounds showed excellent *in vitro* and cellular activity. Compound **4** proved to have the best overall profile with an  $\text{IC}_{50}$  of 2.6 nm, and a combination  $\text{EC}_{50}$  of 1.8  $\mu\text{M}$  in the MTS assay.

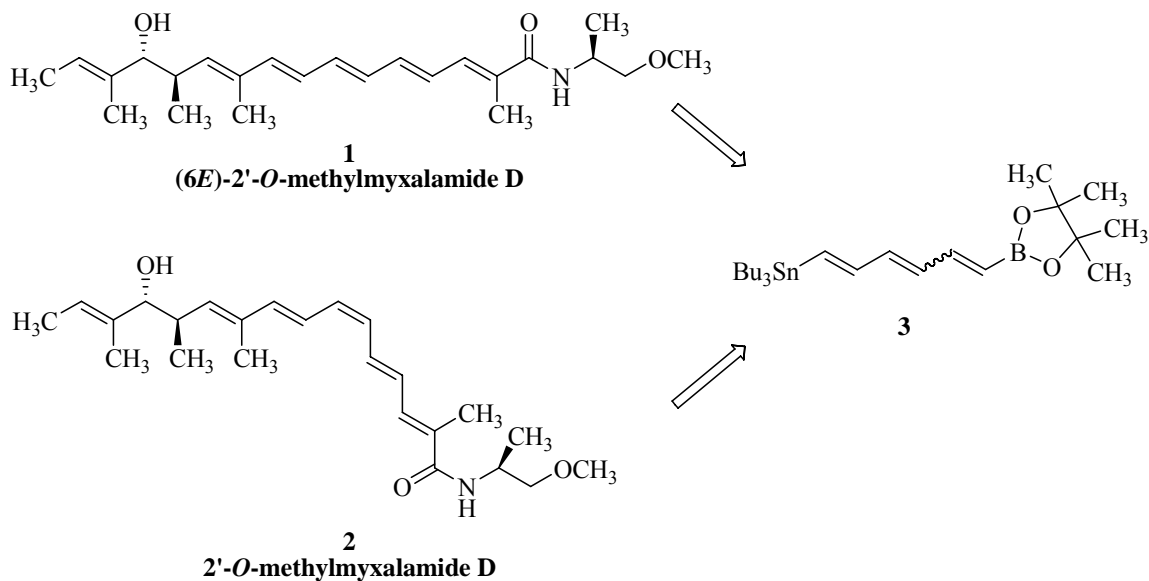
**Figure 2**



**“Total synthesis of polyene natural products using tin/boron linchpin systems.”**

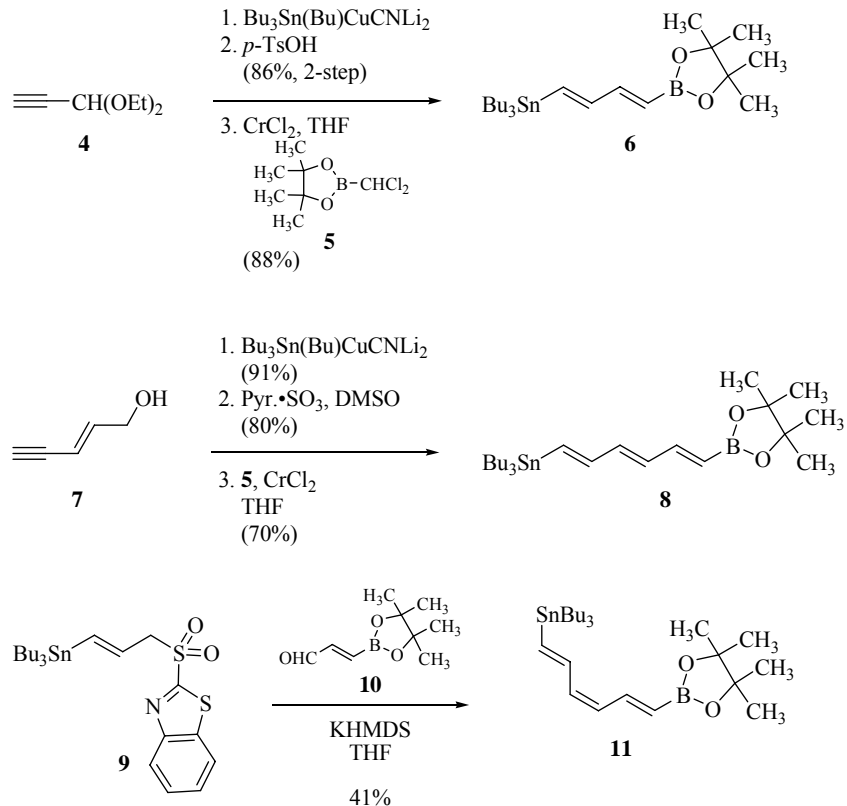
*Robert S. Coleman, (Department of Chemistry, The Ohio State University), Columbus, OH.*

**Figure 1**



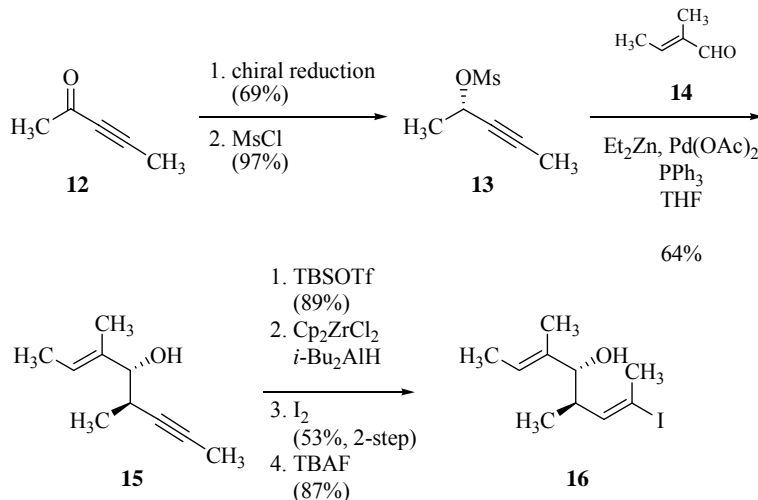
Coleman gave an overview of his “linchpin” strategy culminating in the recent report<sup>1</sup> of the total synthesis of natural products 1 and 2. The strategy utilizes the differing reactivities of tin and boron to selectively incorporate the left- and right-hand portions of the target.

### Scheme 1



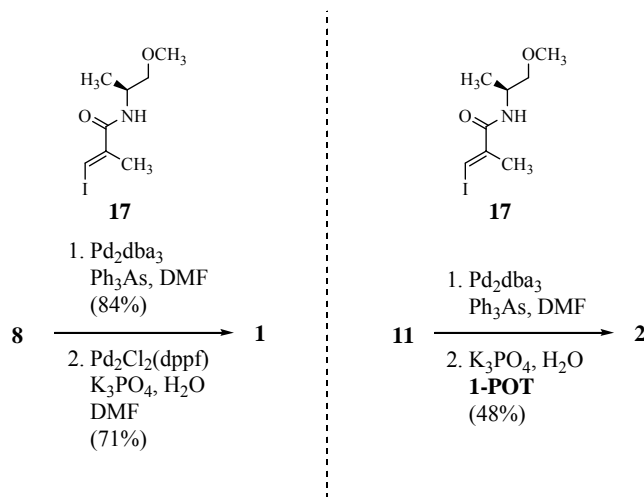
Coleman's first report of the "linchpin" system was diene **6**<sup>2</sup> which was synthesized in 3 steps from commercially available **4** (Scheme 1). The system elegantly exploits boron's need for activation to sequentially and selectively perform a Stille coupling followed by a Suzuki coupling (often in one pot). Coleman used **6** in the syntheses of lucilactaene<sup>3</sup> and gymnoconjugatins A and B.<sup>4</sup> Coleman's talk summarized this methodology, but also highlighted its extension into triene systems **8** and **11** (Scheme 1). The synthesis of **8** is analogous to that of **6** except that the intermediate aldehyde is unmasked by oxidation rather than acetal hydrolysis. The synthesis of **11** relies on the condensation of known stannane **9** and boronate **10** with excellent selectivity (<5% *E*-isomer formed).

## Scheme 2



The synthesis of the left-hand portion of **1** and **2** is shown in Scheme 2. Chiral reduction of **12** followed by mesylation afforded substrate **13** which was substituted with **14** under palladium catalyzed conditions. The divergent intermediate **16** was synthesized from **15** via hydrozirconation and iodination, utilizing a silyl protecting group for the transformation.

## Scheme 3



The completion of the syntheses of **1** and **2** is shown in Scheme 3. Both are accessed divergently from readily available **17**. Compound **1** is synthesized in two steps, with isolation of the intermediate. Compound **2** is synthesized in two steps, however in a one pot procedure. Coleman describes the one-pot procedure for **2** as being optimized for preserving double bond geometry. The reason for the 2-pot procedure in the synthesis of **1** was not discussed, but presumably the yields were significantly higher. The methods described in this discussion represent a clever and useful means for access to traditionally difficult targets. The key intermediates also allow for a great amount of flexibility for use in a medicinal chemistry program.

## References

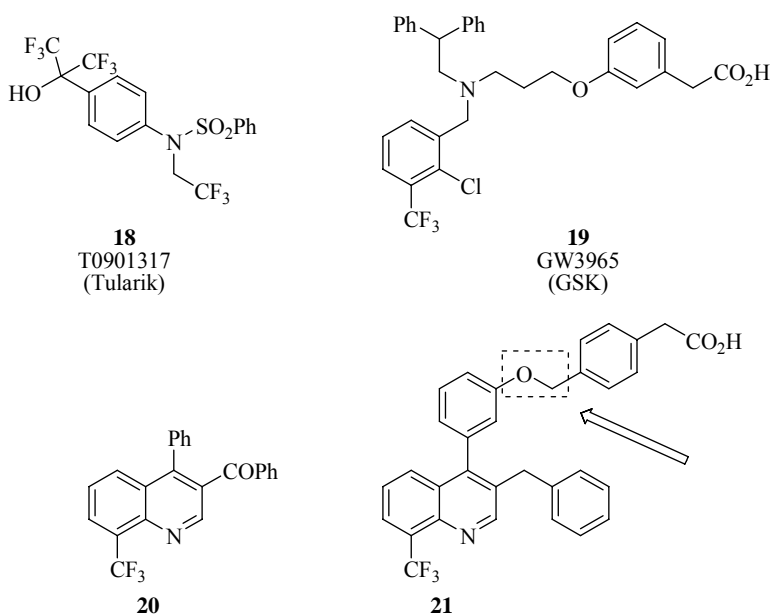
1. Coleman, R. S., Walczak, M. C. *Org. Lett.* **2005**, *7*, 2289-2291.
2. Coleman, R. S., Walczak, M. C. *J. Am. Chem. Soc.* **2005**, *127*, 16038-16039.
3. Coleman, R. S., Walczak, M. C. *J. Org. Chem.* **2006**, *71*, 9841-9844.
4. Coleman, R. S., Walczak, M. C. *J. Org. Chem.* **2006**, *71*, 9841-9844.

---

## “Synthesis and LXR Activity of (4-(3-phenylethynyl)phenyl)quinolones.”

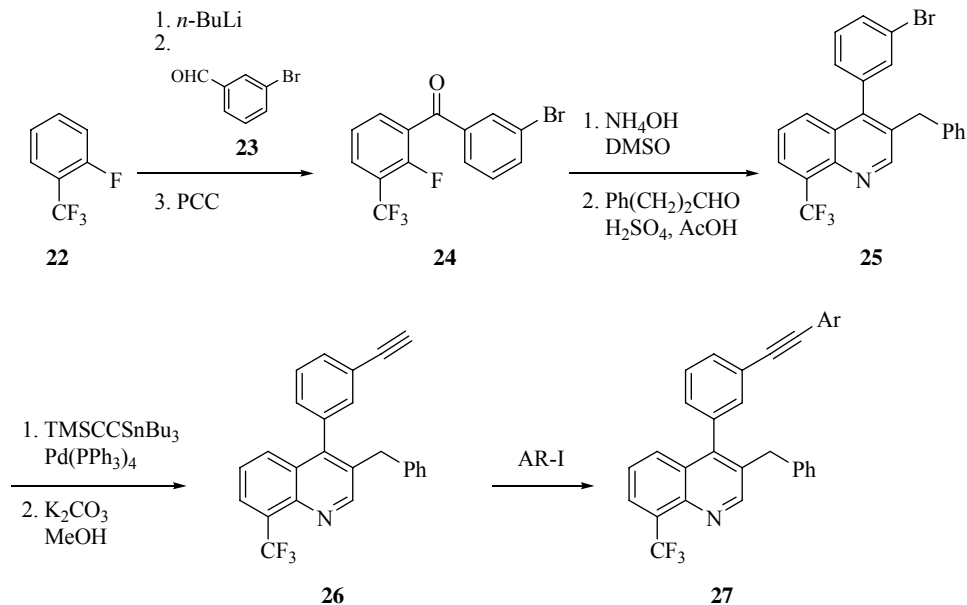
John Ullrich, Robert Morris, Ponnal Nambi, Elaine Quinet, Liang Chen, Anita Halpern, Quang Liu, Dawn Savio, Michael Basso, Ray Unwalla, Anna Wilhelmsson, Annika Goos Nilsson, Crina Ursu, Erik Arnelof, Johnny Sandberg, Cristofer Enroth, Jay Wrobel, (Chemical and Screening Sciences, Cardiovascular and Metabolic Diseases, Structural Biology, Computational Science, Wyeth Research), Collegeville, PA

Figure 1



The authors describe a lead optimization project for the development of a LXR modulator. LXR (Liver X Receptor) is half of a heterodimeric complex that regulates the genes that control LDL (low density lipoprotein) and HDL (high density lipoprotein) metabolism in the body. Agonism of this receptor has been found to be beneficial in reducing LDL serum levels and atherosclerotic lesion area (indicating a lowered risk of cardiovascular disease). The authors cite compounds **18** and **19** (Figure 1) as good examples of LXR modulators (compound **18** is their benchmark for testing). Compound **20** was identified in a high-throughput screen and was used as a core, varying substitution only at the 3- and 4- positions of the quinoline. This poster is a continuation of work presented at the previous years meeting summarizing a hit to lead project that culminated in structures similar to **21**. The authors summarized their efforts to optimize the linker between the phenylacetic acid and the core in order to maximize the interaction between the carboxylate of the ligand and an arginine residue in the binding pocket.

### Scheme 1

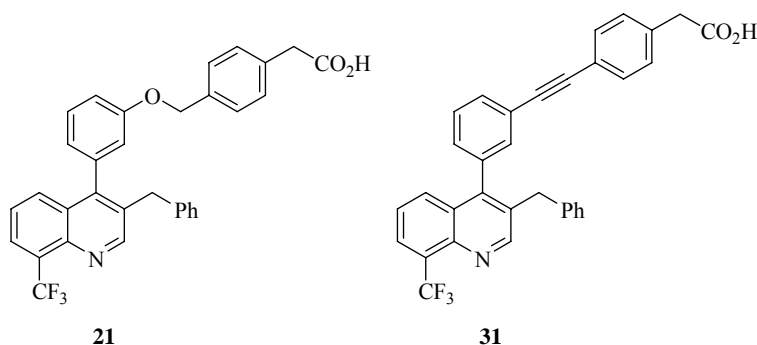


**Table 1**

Compound #	AR	hLXRβ IC <sub>50</sub> (nm)	LAFβ EC <sub>50</sub> (nm)
<b>28</b>	Ph	221	1060
<b>29</b>	4-CO <sub>2</sub> H-Ph	334	513
<b>30</b>	3-CO <sub>2</sub> H-Ph	1043	511
<b>31</b>	<b>4-CH<sub>2</sub>CO<sub>2</sub>H-Ph</b>	<b>8</b>	<b>105</b>
<b>32</b>	3-CH <sub>2</sub> CO <sub>2</sub> H-Ph	14	169
<b>33</b>	4-CH <sub>2</sub> CH <sub>2</sub> CO <sub>2</sub> H-Ph	40	446
<b>34</b>	3-CH <sub>2</sub> CH <sub>2</sub> CO <sub>2</sub> H-Ph	15	134

The preferred spacer described by the authors is an acetylene linker. The synthesis of this class of compounds is described in Scheme 1. Metalation of **22** and condensation with aldehyde **23**, followed by oxidation afforded benzophenone derivative **24**. Displacement of the aryl fluoride with ammonium hydroxide followed by a Friedlander quinoline synthesis afforded bromide **25**. Compound **25** was coupled with TMS protected alkynyl stannane, and then deprotected to afford key intermediate **26**. Sonogashira couplings with a variety of iodides afforded compounds with the general structure **27**. Based on the data from binding and whole-cell assays (Table 1), the authors chose compound **31** as the best in class.

Figure 2



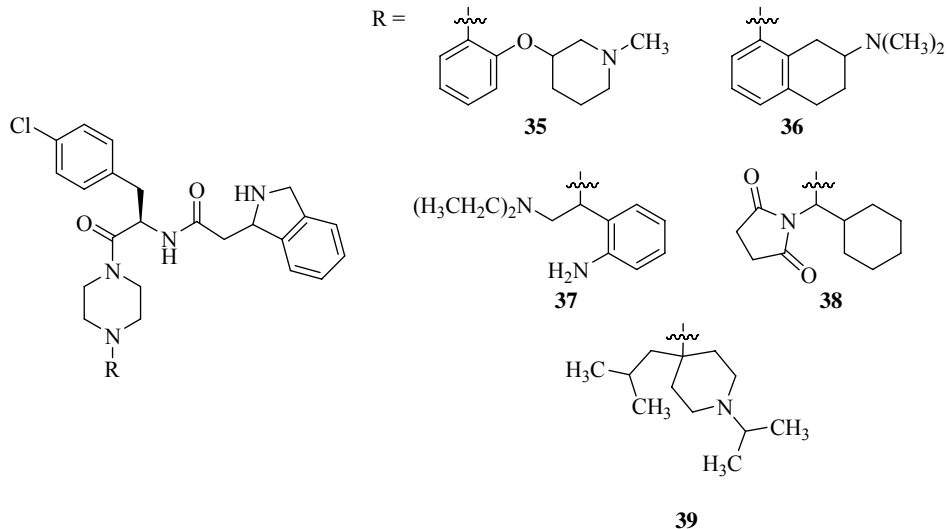
Compound #	LXR $\beta$ IC <sub>50</sub> (nm)	ABCA1 EC <sub>50</sub> (nm)	SREBP1C EC <sub>50</sub> (nm)	cLogP	t <sub>1/2</sub>	AUC	%F
<b>21</b>	2	105	141	7.7	0.25	7270	76
<b>31</b>	<b>8</b>	<b>93</b>	<b>30</b>	<b>8.6</b>	<b>2</b>	<b>38118</b>	<b>99</b>

Compound **31** showed comparable *in vitro* and ABCA1 (gene expression) data with respect to the first generation compound **21** (Figure 2, Wyeth compounds outperform compounds **18** and **19** in these tests). The pharmacokinetic data for the new class of compounds is also improved. However, the data shows a worsening of SREBP1C performance (gene expression assay that should show down-regulation) and the authors reported a disturbing increase in triglyceride levels and liver weight. In summary, the authors have continued to expand upon their quinoline core and have added invaluable information to the structure activity relationship.

**“Design and Biological Evaluation of Small Molecule Ligands for the Melanocortin-4 receptor: *in vivo* Characterization of Potent, Selective MC4R Agonists.”**

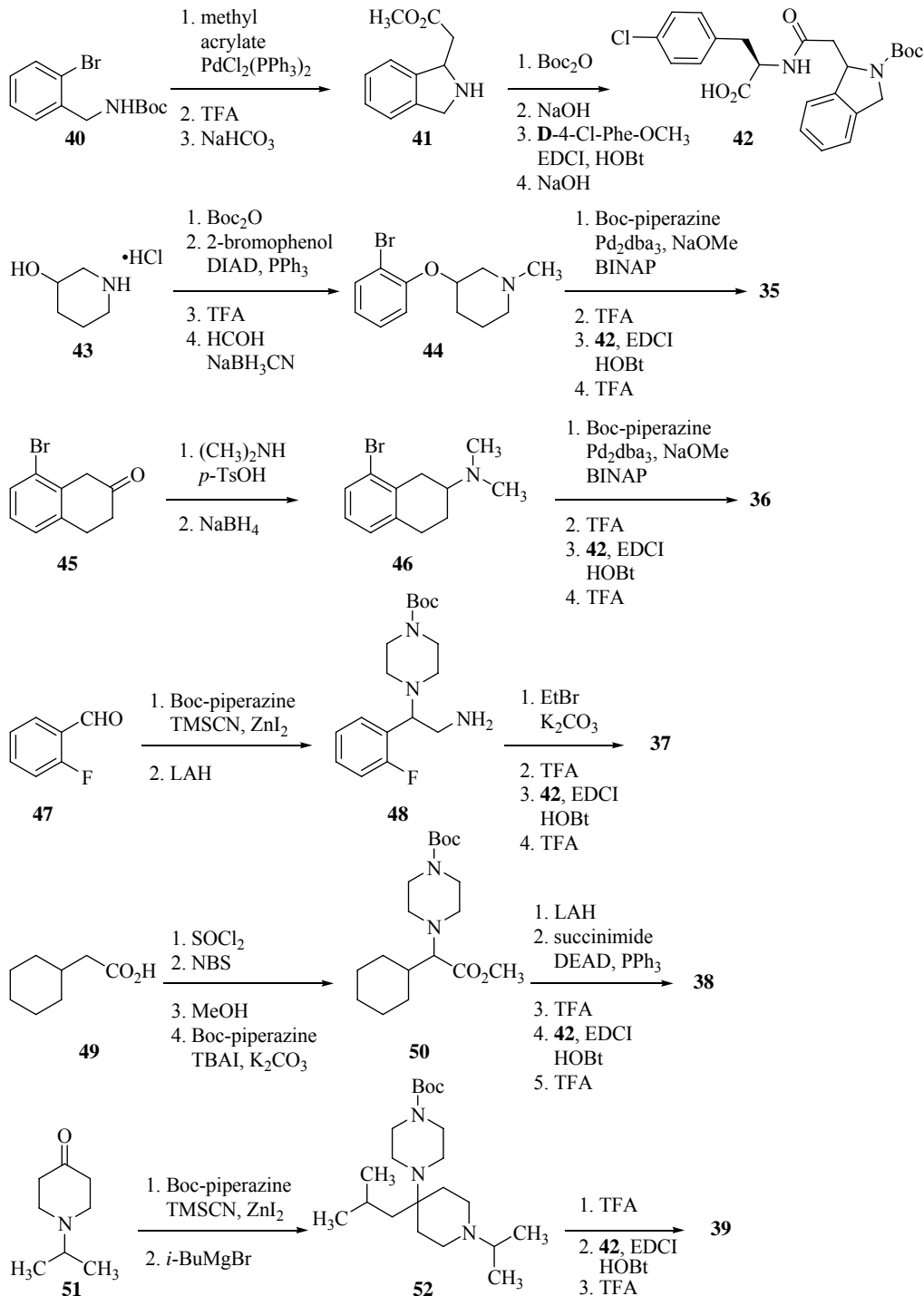
Ryan T. Backer, Karin Briner, Mike P. Clay, Ivan Collado, Libbey S. Craft, Paul J. Emmersion, Matthew J. Fisher, Mark L. Heiman, JeAnne L. Hertel, Saba Husain, Steven L. Kuklish, Terry D. Lindstrom, Ana I. Mateo, Thomas P. O’Brien, Paul L. Omstein, Timothy I. Richardson, Jikesh A. Shah, John M. Zgombick, (Lilly Research Laboratories, Eli Lilly & Company), Indianapolis, IN

**Figure 1**



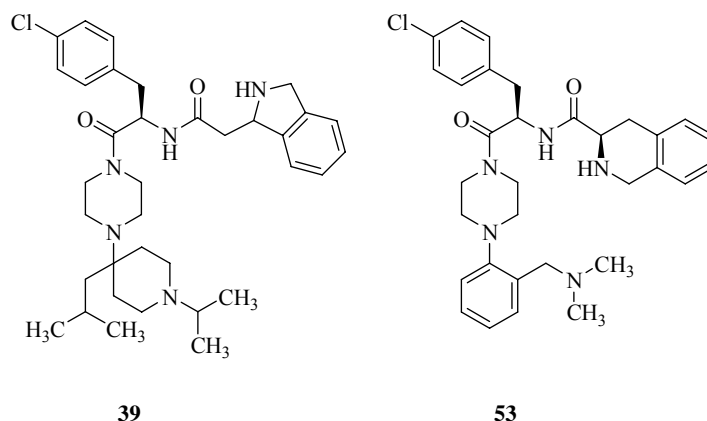
The authors of this poster describe the biological activities of the five compounds shown in Figure 1. The compounds are selective and active agonists for the melanocortin subtype-4 receptor (MC4R), a G-protein-coupled receptor that regulates inflammation, erectile dysfunction and obesity. Treatment with general melanocortin agonists has been shown to decrease food consumption and body mass, however with many side effects. The goal of this project is to expand upon the previously achieved MC4R selectivity to include specificity for treatment of obesity. Rather than targeting pure agonism, the authors are looking for modulation in order to maximize the desired response with respect to the other functions of the receptor. These compounds are derived from a previous generation scaffold described earlier.<sup>1</sup>

### Scheme 1



The synthetic scheme for these scaffolds is shown in Scheme 1. The aryl bromide **40** undergoes a Heck coupling with methyl acrylate followed by Boc-deprotection and intramolecular Michael addition to afford isoindoline **41**. Compound **41** is subjected to a standard protection-deprotection sequence to install the chloro-phenylalanine side chain and afford key intermediate **42**. The five coupling partners are synthesized and coupled to the key intermediate using standard methodology described in Scheme 1.

Figure 2



Compound #	<i>h</i> MC1 <i>K<sub>i</sub></i> (nm)	<i>h</i> MC3 <i>K<sub>i</sub></i> (nm)	<i>h</i> MC4 <i>K<sub>i</sub></i> (nm)	<i>h</i> MC5 <i>K<sub>i</sub></i> (nm)	<i>h</i> MC4 EC <sub>50</sub> (nm)	Fat Utilization (% of control)
$\alpha$ -MSH	---	---	26.6	---	2.56	---
<b>35</b>	1550	2360	69	481	36	94
<b>36</b>	1780	4020	175	267	517	113
<b>37</b>	5960	3420	7	1200	58	112
<b>38</b>	694	358	7	106	5	116
<b>39</b>	1350	954	13	166	4	127
<b>53</b>	20000	7000	60	1400	7	---

Some of the biological data described is shown in Figure 2. The data clearly shows that the compounds are selective for the MC4R receptor over the others in the class and display *in vitro* binding comparable to a natural ligand,  $\alpha$ -MSH. The data also shows that replacement of the aryl-piperazine with various alkyl substituents yields a dramatic improvement in the efficacy of the ligands. Compound **53**,<sup>1</sup> a previous generation analogue shows similar binding and efficacy, better selectivity, but overall poorer performance in PK studies and *in vivo* models. Compound **39** represents the best in class with superior selectivity and efficacy. Compound **39** also shows good clinical efficacy in rats, which displayed increase fat utilization with respect to a placebo and a 67% reduction in food consumption.

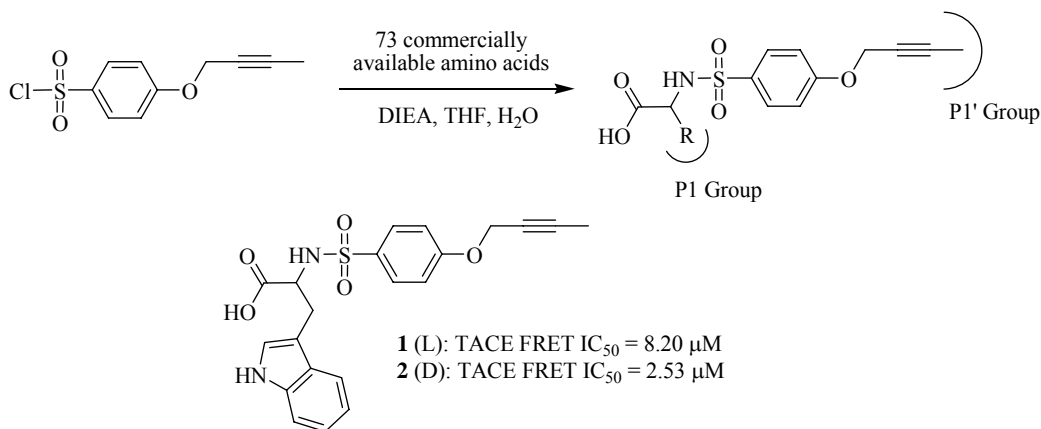
## References

1. Richardson, T. I., Ornstein, P. L., Briner, K., Fisher, M. J., Backer, R. T., Biggers, C. K., Clay, M. P., Emmersion, P. J., Hertel, L. W., Hsiung, H. M., Husain, S., Kahl, S. D., Lee, J. A., Lindstrom, T. D., Martinelli, M. J., Mayer, J. P., Mullaney, J. T., O'Brien, T. P., Pawlak, J. M., Revell, K. D., Shah, J., Zgombick, J. M., Herr, R. J., Melekhov, A, Sampson, P. B., King, C. R. *J. Med. Chem.* **2004**, *47*, 744-755.

**“Design and Synthesis of Tryptophan Butynyloxy Carboxylate Derivatives as TACE Inhibitors”** Kaapjoo Park, Jeremy I. Levin, Alexis Ablasca, Ariamala Gopalsamy, John W. Ellingboe, Weixin Xu, LinHong Sun and Yuhua Zhang (Wyeth Research, Cambridge, MA 02140)

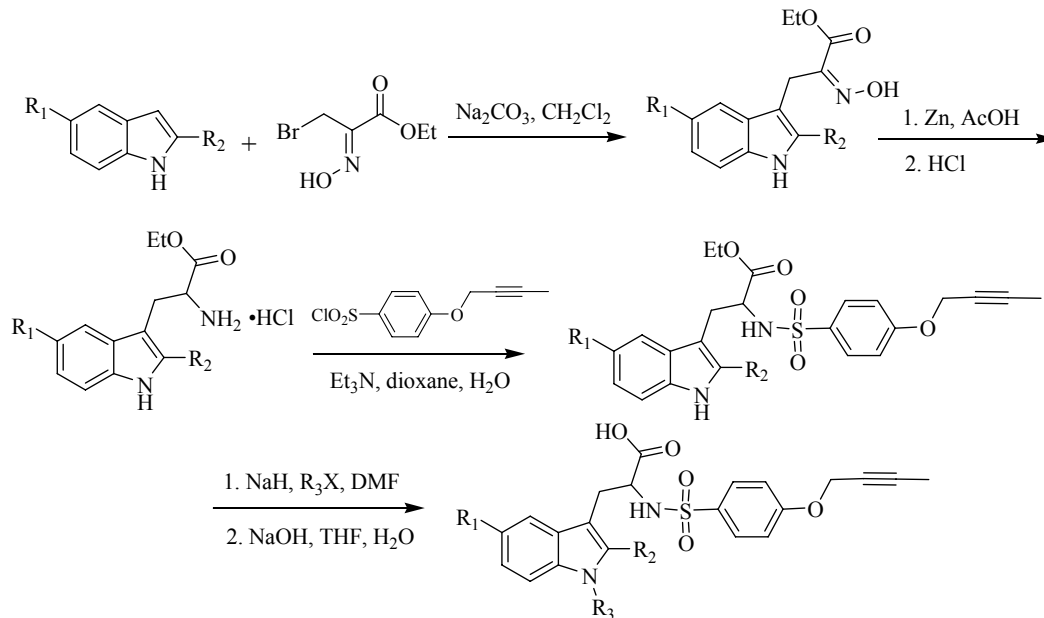
TACE (TNF- $\alpha$  converting enzyme), a member of the ADAM (a disintegrin and metalloprotease-containing enzyme) family of proteases, is responsible for cleaving 26 kDa membrane-bound TNF- $\alpha$  (tumor necrosis factor- $\alpha$ ) to generate 17 kDa soluble TNF- $\alpha$ , a pro-inflammatory cytokine.<sup>1</sup> It has been reported that TNF- $\alpha$  plays a pivotal role in rheumatoid arthritis (RA)<sup>2</sup> and that elevated concentrations of soluble TNF- $\alpha$  are found in the synovial fluid of RA patients.<sup>3</sup> Drugs such as etanercept (Enbrel<sup>®</sup>),<sup>4</sup> a soluble TNF- $\alpha$  receptor, and infliximab (Remicade<sup>®</sup>),<sup>5</sup> an anti-TNF- $\alpha$  antibody, have been used effectively to treat RA patients. However, these drugs have limitations including the need for administration by infusion or parenteral injection. Hence the development of orally active small molecule TACE inhibitors is a highly desirable goal for the treatment of RA.

**Scheme 1**



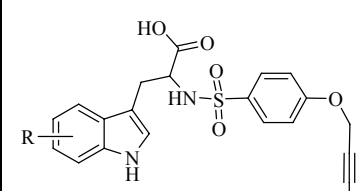
With this goal in mind, Dr. Park and his co-workers synthesized a variety of tryptophan butynyloxy carboxylates. These compounds were prepared by the reaction of various tryptophan derivatives with 4-butynyloxyphenyl sulfonyl chloride as shown in Scheme 1. They found that (D)-2-(4-(but-2-ynyloxy)phenylsulfonamido)-3-(1*H*-indol-3-yl)propanoic acid **2** is more potent than the (L)-isomer **1** and this was used as their lead compound to further optimize a series of tryptophan butynyloxy carboxylates. Scheme 2 described the preparation of these compounds where they modified the P1 group but keeping the P1' group constant.

### Scheme 2



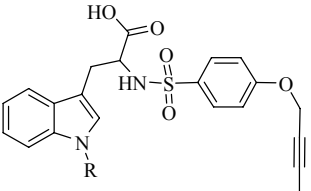
The summary of their *in vitro* SAR studies are shown in Table 1, Table 2 and Table 3.

**Table 1.** Mono-substituted Indole (P1) Carboxylic Acids

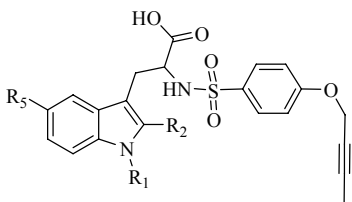
	Comps	R	TACE IC <sub>50</sub> (μM)
	<b>1</b>	H (L)	8.20
<b>2</b>	H (D)	2.53	
<b>3</b>	5-Me (L)	27% <sup>a</sup>	
<b>4</b>	5-Me (D)	0.14	
<b>5</b>	5-MeO (L)	10.1	
<b>6</b>	5-MeO (D)	0.14	
<b>7</b>	5-BnO (L)	6.98	
<b>8</b>	5-BnO (D)	0.37	
<b>9</b>	5-F	1.56	
<b>10</b>	5-OH	1.61	
<b>11</b>	5-Br	0.63	
<b>12</b>	6-F	2.96	
<b>13</b>	6-Me	1.57	
<b>14</b>	6-OH (L)	1.57	

<sup>a</sup> % inhibition at 1 μM

**Table 2.** *N*-Substituted Indole (P1) Carboxylic Acids

	Compds	R	D/L	TACE IC <sub>50</sub> (μM)
	<b>2</b>	H (D)	H (D)	D
<b>15</b>	Boc	Boc	D	3.67
<b>16</b>	Me	Me	D	1.43
<b>17</b>	<i>n</i> -pentyl	<i>n</i> -pentyl	D	2.31
<b>18</b>	Cyclohexyl-methyl	Cyclohexyl-methyl	D	1.71
<b>19</b>	4-PhO-Bu	4-PhO-Bu	D	1.25
<b>20</b>	Bn	Bn	D	2.15
<b>21</b>	<i>O</i> -Ph-Bn	<i>O</i> -Ph-Bn	D	0.97
<b>22</b>	<i>p</i> -allyloxy-Bn	<i>p</i> -allyloxy-Bn	D	0.54
<b>23</b>	3,5-dimethoxy-Bn	3,5-dimethoxy-Bn	D	0.98
<b>24</b>	<i>o</i> -CF <sub>3</sub> -Bn	<i>o</i> -CF <sub>3</sub> -Bn	D	2.4% <sup>a</sup>
<b>25</b>	<i>m</i> -CF <sub>3</sub> -Bn	<i>m</i> -CF <sub>3</sub> -Bn	D	2.30
<b>26</b>	<i>p</i> -CF <sub>3</sub> -Bn	<i>p</i> -CF <sub>3</sub> -Bn	D	4.40
<b>27</b>	<i>p</i> -Me-Bn	<i>p</i> -Me-Bn	D	3.59
<b>28</b>	<i>p</i> -F-Bn	<i>p</i> -F-Bn	D	1.90
<b>29</b>	<i>p</i> -Cl-Bn	<i>p</i> -Cl-Bn	D	3.45
<b>30</b>	<i>p</i> -MeO-Bn	<i>p</i> -MeO-Bn	D	0.08
<b>31</b>	<i>p</i> -MeO-Bn	<i>p</i> -MeO-Bn	L	1.18

<sup>a</sup> % inhibition at 1 μM**Table 3.** Di and Tri-substituted Indole (P1) Carboxylic Acids

	Compds	R <sub>2</sub>	R <sub>5</sub>	R <sub>1</sub>	TACE IC <sub>50</sub> (μM)
	<b>32</b>	H	H	CO <sub>2</sub> H	Me or Et
<b>33</b>	H	H	MeO	2-methylpropyl	1.23
<b>34</b>	Me	Me	Cl	2-methylpropyl	0.30
<b>35</b>	H	Me	Me	<i>p</i> -MeO-Bn	0.89
<b>36</b>	Me	Me	Cl	<i>p</i> -MeO-Bn	0.19
<b>37</b>	Me	Me	MeO	Me	62% <sup>a</sup>
<b>38</b>	Me	Me	MeO	Bn	0.25
<b>39</b>	H	Me	MeO	3,4-methylenedioxy-Bn	1.50
<b>40</b>	Me	Me	MeO	3,4-methylenedioxy-Bn	0.33
<b>41</b>	H	Me	MeO	<i>m</i> -MeO-Bn	2.24
<b>42</b>	Me	Me	MeO	<i>m</i> -MeO-Bn	0.28
<b>43</b>	Me	Me	MeO	<i>o</i> -CF <sub>3</sub> -Bn	0.50
<b>44</b>	Me	Me	MeO	<i>p</i> -CF <sub>3</sub> -Bn	0.79
<b>45</b>	H	Me	MeO	<i>o</i> -F-Bn	2.24
<b>46</b>	Me	Me	MeO	<i>o</i> -F-Bn	0.30
<b>47</b>	Me	Me	MeO	<i>m</i> -F-Bn	0.34
<b>48</b>	Me	Me	MeO	<i>p</i> -F-Bn	0.32
<b>49</b>	Me	Me	MeO	<i>p</i> -Cl-Bn	0.29
<b>50</b>	Me	Me	Cl	<i>p</i> -Cl-Bn	0.33
<b>51</b>	Me	Me	MeO	<i>m</i> -CN-Bn	0.41
<b>52</b>	Me	Me	MeO	<i>p</i> -CN-Bn	0.47

<sup>a</sup> % inhibition at 1 μM

**Table 4.** MMP and Cell-Based Activity

Compds	MMP-1	MMP-2	MMP-13	MMP-14	TACE	Raw Cells
	IC <sub>50</sub> (μM)	IC <sub>50</sub> (μM)	IC <sub>50</sub> (μM)	IC <sub>50</sub> (μM)	IC <sub>50</sub> (μM)	IC <sub>50</sub> (μM)
<b>4</b>	>50	0.27	1.81	6.82	0.14	7.8
<b>6</b>	>50	1.27	13.6	20.7	0.14	57
<b>8</b>	>50	3.27	4.44	19.7	0.37	NT
<b>30</b>	>50	1.44	4.56	13.0	0.08	Inactive

In summary the most potent tryptophan carboxylates in the TACE FRET assay are compounds **4**, **6** and **30**. However, these compounds are not very potent in Raw cells assay. The best tryptophan carboxylate **4** has an IC<sub>50</sub> of 7.8 μM in Raw Cells (Table 4).

### References

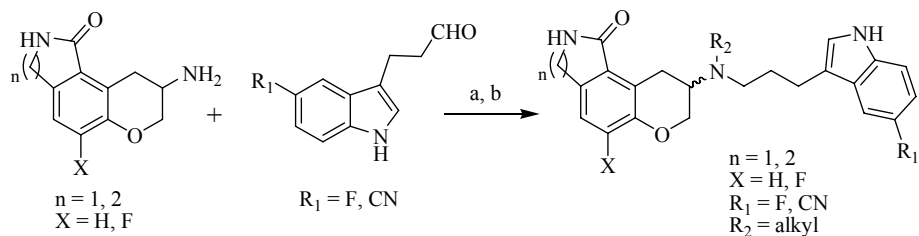
1. L. Killar, J. White, R. Black and J. Peschon, *Ann. N.Y. Acad. Sci.* **1999**, 878, 442.
2. (a) L. Roberts and G.J. McColl, *Intern. Med. J.* **2004**, 34, 687; (b) K.L. Hyrich, A.J. Silman, K.D. Watson and D. P.M. Symmons, *Ann. Rheum. Dis.* **2004**, 63, 1538; (c) M. Feldmann and R.N. Maini, *Annu. Rev. Immunol.* **2001**, 19, 163.
3. M. Feldmann, F.M. Brennan, B.M. Foxwell and R.N. Maaini, *Curr. Dir. Autoimmun.* **2001**, 3, 188.
4. (a) G. Kobelt, P. Lindgren, A. Singh and L. Klareskog, *Ann. Rheum. Dis.* **2005**, 64, 1174; (b) S.W. Baumgartner, R.M. Fleischmann, L.W. Moreland, M.H. Schiff, J. Markenson and J.B. Whitmore, *J. Rheumatol.* **2004**, 31, 1532; (c) L. Terslev, S. Torp-Pedersen, E. Qvistgaard, H. Kristoffersen, H. Rogind, B. Danneskiold-Samsoe and H. Bliddal, *Ann. Rheum. Dis.* **2003**, 62, 178.
5. (a) M. Asif, A. Siddiqui and L.J. Scott, *Drugs* **2005**, 65, 2179; (b) A. Familian, A.E. Voskuyl, G.J. van Mierlo, H.A. Heijst, J.W.R. Twisk, B.A.C. Dijkmans and C.E. Hack, *Ann. Rheum. Dis.* **2005**, 64, 1003; (c) E.W. St Clair, D.M.F.M. van der Heijde, J.S. Smolen, R.N. Maini, J.M. Bathon, P. Emery, E. Keystone, M. Shiff, J.R. Kalden, B. Wang, K. de Woody, R. Weiss and D. Baker, *Arthritis Rheum.* **2004**, 50, 3432.

### “Synthesis and SAR Evaluation of Lactam-Fused Chroman Derivatives Having Dual Affinity at Serotonin 5-HT<sub>1A</sub> Receptor and Serotonin Transporter”

Zhongqi Shen, Nicole T. Hatzenbuehler, Deborah A. Evrard, Michael Chlenov, Boyd L. Harrison, Ronald L. Magolda, Magid Abou-Gharbia, Geoffrey Hornby, Deborah L. Smith, Kelly M. Sullivan, Lee E. Schechter, Terrance H. Andree and P. Siva Ramamoorthy (Wyeth Research, Princeton, NJ 08543)

Selective serotonin reuptake inhibitors (SSRIs) have become a primary mode of therapy for the treatment of depression due to fewer side effects than the traditional tricyclics, but they suffer from delayed onset of action (2–3 weeks).<sup>1</sup> This onset delay is the result of activation of 5-HT<sub>1A</sub> autoreceptors that reduce cell-firing activity. Data suggest that co-administration of a 5HT<sub>1A</sub> receptor antagonist and a 5-HT reuptake site antagonist could accelerate antidepressant effects.<sup>2–3</sup> With this data in mind, Dr Shen and his co-workers developed dual acting molecules that block both the 5-HT<sub>1A</sub> receptor and 5HT reuptake site. He described in his poster the synthesis and evaluation of a series of lactam-fused 3-aminochromans as combined 5-HT<sub>1A</sub>/SSRI antagonists (Scheme 1).

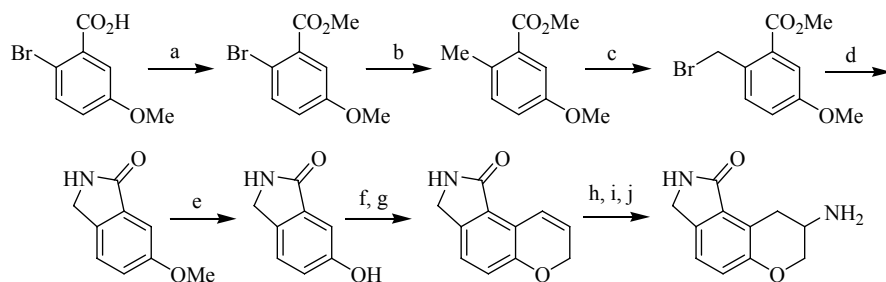
### Scheme 1



Reagents and Conditions: (a)  $\text{NaBH}_3\text{CN}$ , AcOH, MeOH; (b) aldehyde or ketone,  $\text{NaBH}_3\text{CN}$ , AcOH, MeOH.

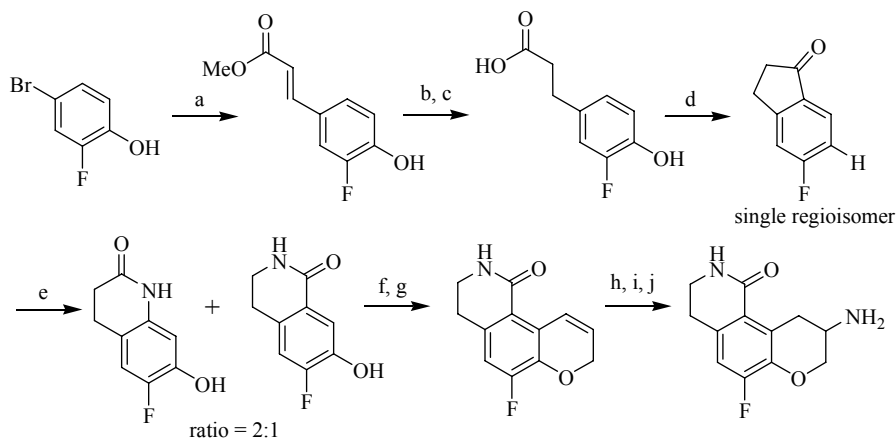
The syntheses of 5-membered and 6-membered lactams are shown in Schemes 2, 3 and 4. The aldehyde was prepared in 2 steps from 4-substituted phenylhydrazine as depicted in Scheme 5.

### Scheme 2



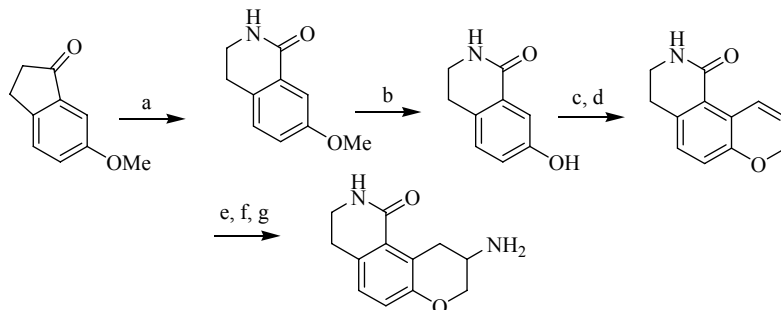
Reagents and Conditions: (a) MeI, DBU, MeCN; (b)  $\text{Me}_2\text{Zn}$ ,  $\text{Cl}_2\text{Ni}(\text{PPh}_3)_2\text{Me}_2$ , DMF; (c) NBS, AIBN, benzene; (d)  $\text{NH}_3$ , MeOH; (e)  $\text{BBr}_3$ ,  $\text{CH}_2\text{Cl}_2$ ; (f) propargyl bromide,  $\text{K}_2\text{CO}_3$ ; (g) diethylaniline, 210 °C; (h)  $\text{NaNO}_2$ ,  $\text{I}_2$ , NMP; (i)  $\text{NaBH}_4$ ,  $\text{SiO}_2$ ,  $\text{CHCl}_3$ ; (j)  $\text{NH}_2\text{NH}_2$ , Raney Ni, EtOH.

### Scheme 3



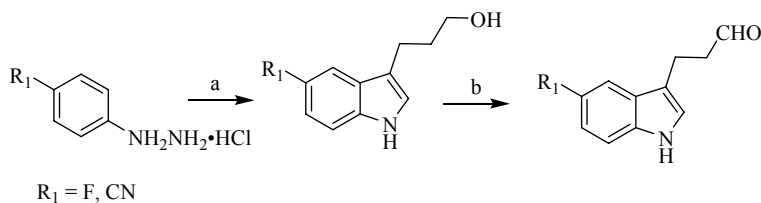
Reagents and Conditions: (a) Methyl acrylate,  $\text{Pd}(\text{OAc})_2$ , tri-*o*-tolylphosphine,  $\text{Et}_3\text{N}$ , DMF; (b)  $\text{H}_2$ , Pd/C, MeOH; (c) LiOH, MeOH, THF,  $\text{H}_2\text{O}$ ; (d)  $\text{AlCl}_3$ , NaCl, 180 °C; (e) MsOH,  $\text{NaN}_3$ ,  $\text{CHCl}_3$ ; (f) propargyl bromide,  $\text{K}_2\text{CO}_3$ ; (g) diethylaniline, 210 °C; (h)  $\text{NaNO}_2$ ,  $\text{I}_2$ , NMP; (i)  $\text{NaBH}_4$ ,  $\text{SiO}_2$ ,  $\text{CHCl}_3$ ; (j)  $\text{NH}_2\text{NH}_2$ , Raney Ni, EtOH.

### Scheme 4



Reagents and Conditions: (a) MsOH, NaN<sub>3</sub>, CHCl<sub>3</sub>; (b) BBr<sub>3</sub>, CH<sub>2</sub>Cl<sub>2</sub>; (c) propargyl bromide, K<sub>2</sub>CO<sub>3</sub>; (d) diethylaniline, 210 °C; (e) NaNO<sub>2</sub>, I<sub>2</sub>, NMP; (f) NaBH<sub>4</sub>, SiO<sub>2</sub>, CHCl<sub>3</sub>; (g) NH<sub>2</sub>NH<sub>2</sub>, Raney Ni, EtOH.

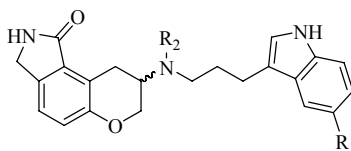
### Scheme 5



Reagents and Conditions: (a) 3,4-dihydro-2H-pyran, dioxane, H<sub>2</sub>O; (b) DCC, Et<sub>3</sub>N, DMSO.

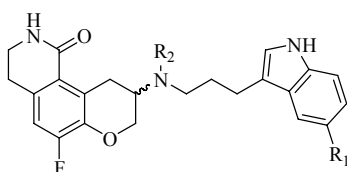
The biological data for these compounds are presented in Tables 1, 2 and 3.

**Table 1.** Data for 5-Membered Lactams



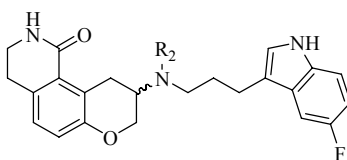
Compounds	R <sub>1</sub>	R <sub>2</sub>	stereo	5-HT <sub>1A</sub> Ki (nM)	5-HT-t Ki (nM)	cAMP EC <sub>50</sub> (nM)	cAMP EC <sub>50</sub> (nM)
<b>1</b>	F	H	rac	24	2	61	100
<b>2</b>	F	Me	rac	22	8	75	80
<b>3</b>	F	Et	rac	2	2	28	78
<b>4</b>	F	MecPr*	rac	6	1	IC <sub>50</sub> = 223	0
<b>5</b>	F	MecPr*	(-)	3	6	IC <sub>50</sub> = 320	0
<b>6</b>	F	MecPr*	(+)	3	1.5	24	84
<b>7</b>	F	<i>c</i> -Bu	rac	101	7	350	NT
<b>8</b>	F	<i>i</i> -Bu	rac	NT	17	NT	NT
<b>9</b>	F	MecHex*	rac	NT	89	NT	NT
<b>10</b>	F	Bz	rac	85	10	436	96
<b>11</b>	CN	H	rac	36	1	22	91
<b>12</b>	CN	MecPr*	rac	4	3	IC <sub>50</sub> = 63	0
<b>13</b>	CN	MecPr*	(-)	10	3	IC <sub>50</sub> = 203	0
<b>14</b>	CN	MecPr*	(+)	31	3	19	100

\* MecPr = cyclopropylmethyl; MecHex = cyclohexylmethyl

**Table 2.** Data for 10-Fluoro Substituted 6-Membered Lactams

Compounds	R <sub>1</sub>	R <sub>2</sub>	stereo	5-HT <sub>1A</sub> K <sub>i</sub> (nM)	5-HT-t K <sub>i</sub> (nM)	cAMP EC <sub>50</sub> (nM)	cAMP EC <sub>50</sub> (nM)
<b>15</b>	F	H	rac	6	1	4	98
<b>16</b>	F	Et	rac	4	1	10	92
<b>17</b>	F	MecPr*	rac	50	52	101	62

\* MecPr = cyclopropylmethyl

**Table 3.** Data for Des-Fluoro Substituted 6-Membered Lactams

Compounds	R <sub>2</sub>	stereo	5-HT <sub>1A</sub> K <sub>i</sub> (nM)	5-HT-t K <sub>i</sub> (nM)	cAMP EC <sub>50</sub> (nM)	cAMP EC <sub>50</sub> (nM)
<b>18</b>	H	rac	44	1	25	87
<b>19</b>	Me	rac	23	4	26	99
<b>20</b>	Et	rac	6	7	9	97
<b>21</b>	<i>n</i> -Pr	rac	13	10	34	100
<b>22</b>	<i>i</i> -Pr	rac	129	4	252	94
<b>23</b>	MecPr*	rac	19	2	36	91
<b>24</b>	<i>i</i> -Bu	rac	927	31	NT	NT
<b>25</b>	<i>c</i> -Bu	rac	95	2	95	28
<b>26</b>	(CH <sub>2</sub> ) <sub>2</sub> CF <sub>3</sub>	rac	966	209	NT	NT
<b>27</b>	Bz	rac	1220	120	NT	NT

\* MecPr = cyclopropylmethyl

In the fluoro-substituted 6-membered lactam series, 5-HT<sub>1A</sub> affinity is sensitive to the size of the R<sub>2</sub> group (Table 2). The secondary amine (compd **15**) displayed similar affinity as the tertiary amine possessing an ethyl group (compd **16**). In the desfluoro 6-membered lactams, tertiary amines possessing small alkyl groups (Compds **19–21**, **23**) displayed somewhat greater 5-HT<sub>1A</sub> affinity than secondary amines (compd **18**). However, branched alkyl groups and a benzyl group in the R<sub>2</sub> position reduced 5-HT<sub>1A</sub> affinity (Table 3). In general, the presence of the 5-membered ring lactam promoted 5-HT<sub>1A</sub> affinity (Table 1). In the 5-membered lactam series, 5-HT<sub>1A</sub> antagonist intrinsic activity appears to reside in the (–) enantiomers (Compds **5** and **13**).

## References

1. Blier, P.; Bergeron, R. *J. Clin. Psychiatry* **1998**, *suppl. 5*, 16
2. Artigas, F.; Perez, V.; Alvarez, E. *Arch. Gen. Psychiatry* **1994**, *51*, 248
3. Blier, P.; Bergeron, R. *J. Clin. Psychopharmacology* **1995**, *15*, 217.

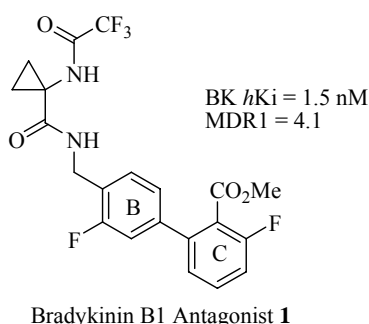
---

**“Development of Cyclopropylcarboxamide Bradykinin B<sub>1</sub> Receptor Antagonists with Modified Biphenyl Motifs”**, Ronald K. Chang, Christina N. Di Marco, Kathy L. Murphy, Richard W. Ransom, Duane R. Reiss, Cuyue Tang, Thomayant Prueksaritanont, Douglas J. Pettibone, Mark G. Bock and Scott D. Kuduk (Merck Research Laboratories, West Point, PA 19486).

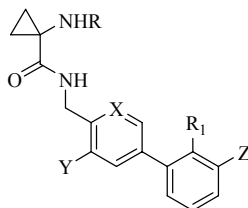
Despite a growing demand for new analgesics to alleviate pain, new approaches and medications to address this medical need has remained unmet. One approach to pain treatment is development of bradykinin B<sub>1</sub> antagonists as a novel way to treat chronic inflammatory pain. Bradykinin B<sub>1</sub> antagonists have been shown to attenuate late phase hyperalgesia during prolonged chronic pain and inflammation.<sup>1</sup> In addition, bradykinin B<sub>1</sub> receptors are constitutively expressed in the central nervous system of rats and mice, broadening the therapeutic potential of bradykinin B<sub>1</sub> receptor antagonists for mediating chronic pain and inflammation.<sup>2</sup>

Dr Chang previously disclosed a variety of aminocyclopropane carboxamide analogs as small-molecule, non-peptide bradykinin B<sub>1</sub> receptor antagonists (Figure 1).<sup>3</sup> Initial SAR studies focused on improving receptor affinity, physical properties and pharmacokinetics while minimizing P-glycoprotein efflux (P-gp).

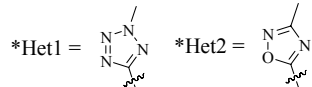
**Figure 1**



Here in this report, Dr Chang presented a refinement of the biphenyl backbone via installation of a nitrogen into the B-ring and halogens to B- and C-rings, as well as incorporation of heterocyclic methyl ester surrogates with the goal of improving pharmacokinetics, while maintaining high B<sub>1</sub> receptor affinity. The biological data for these compounds are shown in Table 1.

**Table 1**

Compds	R	R <sub>1</sub>	X	Y	Z	<i>hK</i> <sub>1</sub> (nM) <sup>a</sup>	MDR <sub>1</sub> <sup>b</sup>	LogP	PB(%) <sup>c</sup>
<b>1</b>	COCF <sub>3</sub>	CO <sub>2</sub> Me	CH	F	F	1.5	4.1	2.7	92
<b>2a</b>	COCF <sub>3</sub>	CO <sub>2</sub> Me	N	F	F	1.5	3.1	2.3	69
<b>2b</b>	COCF <sub>3</sub>	CO <sub>2</sub> Me	N	F	Cl	1.3	3.1	2.2	NT
<b>2c</b>	COCF <sub>3</sub>	CO <sub>2</sub> Me	N	Cl	F	2.0	3.1	2.8	90
<b>2d</b>	COCF <sub>3</sub>	CO <sub>2</sub> Me	N	Cl	Cl	2.3	3.0	3.2	95
<b>3a</b>	COCF <sub>3</sub>	Het1 *	N	F	F	1.4	6.5	1.8	77
<b>3b</b>	COCF <sub>3</sub>	Het1 *	N	Cl	Cl	1.2	6.0	2.7	89
<b>3c</b>	COCF <sub>3</sub>	Het1 *	N	Cl	F	1.0	5.2	2.4	84
<b>3d</b>	COCF <sub>2</sub> Cl	Het1 *	N	Cl	F	2.2	5.7	2.8	91
<b>3e</b>	COCF <sub>2</sub> H	Het1 *	N	Cl	F	1.5	6.2	1.8	81
<b>4</b>	COCF <sub>3</sub>	Het2*	N	Cl	F	0.85	3.9	2.7	89



a = values represent the numerical average of at least 2 experiments.

b = MDR<sub>1</sub> Directional Transport Ratio (B to A)/(A to B); values represent the average of 3 experiments.

c = Protein binding was measured using 10%HSA.

Compound **1** has a good B<sub>1</sub> affinity (1.5 nM) and a moderate P-gp efflux ratio of 4.1. To enhance the physical properties of **1**, a basic, pyridyl nitrogen was introduced into the B-ring, with the goal of lowering log P and protein binding (PB). The pyridine B-ring (**2a–d**) helped lower P-gp efflux, while maintaining high receptor binding affinity. Compound **2a**, containing a fluoride atom in both B- and C-rings, exhibited a lower Log P and a significantly lower PB value relative to **1**. Compounds **2c** and **2d**, both containing a chlorine atom in the B-ring, had physical properties similar to **1**. Introduction of a 2-methyltetrazole to the C-ring maintained high affinity but increased P-gp efflux (**3a–e**). Adjustments to the amide R group in compounds **3d–e** did little to improve potency and MDR<sub>1</sub> values. Replacing methyl ester with 3-methyl-1,2,4-oxadiazole (**4**) enhanced affinity for the hB<sub>1</sub> receptor, lower P-gp efflux and possessed comparable physical properties to **1**. Dog and rat pharmacokinetic data for select compounds are shown in Table 2.

**Table 2**

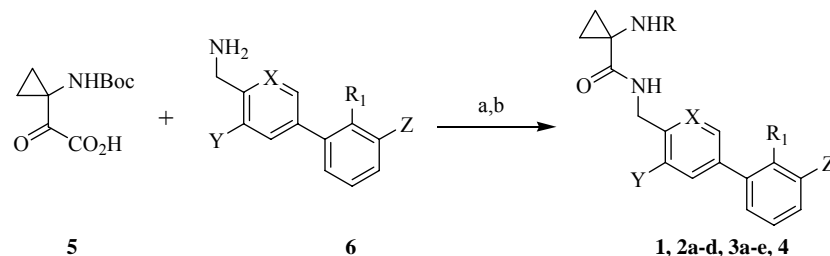
Compds	Dog F <sup>a</sup> %	Dog t <sub>1/2</sub> hr	Dog Cl mL/min/Kg	Dog Vd L/Kg	Rat F <sup>b</sup> %	Rat t <sub>1/2</sub> hr	Rat Cl mL/min/Kg	Rat Vd L/Kg
<b>1</b>	NT	0.98	18	0.90	35	1.0	7.6	0.37
<b>2a</b>	NT	NT	NT	NT	66	1.0	8.5	0.28
<b>3b</b>	NT	0.76	8.9	0.42	21	4.6	1.5	0.44
<b>3c</b>	42	0.70	4.8	0.27	40	8.6	0.44	0.31
<b>4</b>	NT	1.1	12	0.74	33	1.7	4.4	0.38

a = mongrel dogs (n=2); Oral dose = 3 mg/Kg; IV dose = 1 mg/Kg

b = sprague-dawley rats (n = 3); oral dose = 10 mg/Kg; IV dose = 2 mg/Kg

The biphenylamine methyl ester **1** exhibited a short half-life with elevated clearance in both dog and rats. The B-ring pyridine replacement (**2a**) had a similar rat half-life and clearance but a ~2 fold improvement in bioavailability relative to **1**. Incorporation of a B-ring pyridine and replacement of a the labile methyl ester with a 2-methyltetrazole (**3b–c**) provided an overall improvement in PK profile with lowered clearance in both dog and rat with higher rat half-lives of 4.6 and 8.6 hours, respectively. The oxadiazole **4** possessed similar dog and rat PK profiles to compound **1**, with slightly lowered clearance in both species.

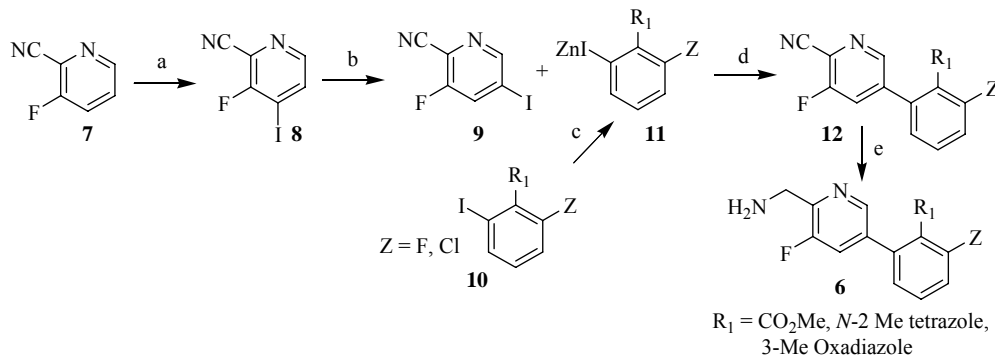
The synthesis of these compounds is shown in Scheme 1, in which the common intermediate **6** underwent acylation with acid **5**, *N*-Boc deprotection and then acylation with the appropriate acids provided the desired BK B<sub>1</sub> receptor antagonists (**1**, **2a–d**, **3a–e**, **4**).

**Scheme 1**

Reagents and Conditions: (a) EDC, HOBT, TEA, DMF; (b) RCO<sub>2</sub>H, EDC, HOBT, TEA, DMF

The intermediate **6** was prepared using two routes as depicted in Schemes 2 and 3. Metalation of **7** with LDA and trapping with iodine provided **8**. Treatment of **8** with LDA smoothly induced a 1,2-migration of the iodide from 4- to 5-position (halogen dance) to give **9**. Negishi coupling with arylzincate **11** and subsequent reduction gave amine **6** (Y = F, Scheme 2).

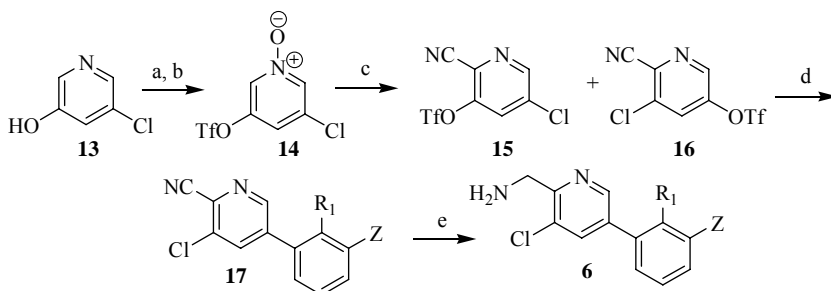
### Scheme 2



Reagents and Conditions: (a) LDA, I<sub>2</sub>, THF; (b) LDA, THF; (c) Rieke Zn, Pd(PPh<sub>3</sub>)<sub>4</sub>, (d) THF; 80 °C; (e) Raney Ni, NH<sub>3</sub>, MeOH.

The second route involves the conversion of a hydroxyl group in **13** to a triflate, followed by *N*-oxidation to give **14**. Cyanation provided an inseparable mixture (2:5) of regioisomers **15** and **16**, which were subjected to Negishi cross-coupling conditions with arylzincate **11**. The resulting mixture was separated to provide **17**, which was reduced to the amine **6** (R = Cl, Scheme 3).

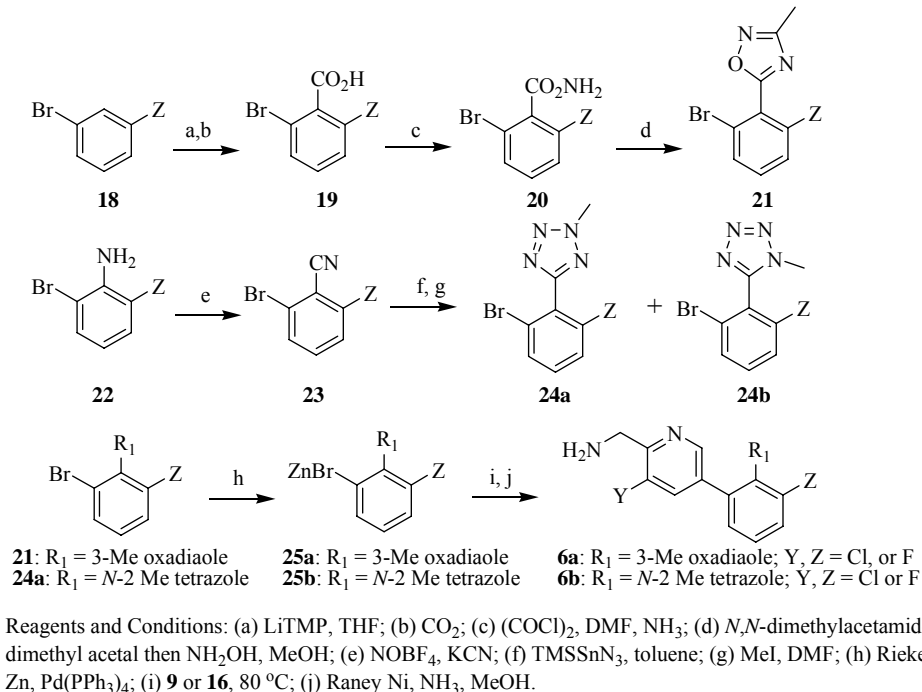
### Scheme 3



Reagents and Conditions: (a) Tf<sub>2</sub>O; (b) *m*-CPBA; (c) TMSCN; (d) **11**, 80 °C; (e) Raney Ni, NH<sub>3</sub>, MeOH.

The synthesis of the heterocyclic methyl ester surrogates are shown in Scheme 4. *Ortho*-lithiation of **18**, anion trapping with carbon dioxide and subsequent acidic workup afforded acid **19**. Treatment of **19** with oxalyl chloride followed by reaction with ammonia gas gave amide **20** which was then converted to 1,2,4-oxadiazole **21** in a two step one pot reaction. *N*-2-Methyltetrazole **24a** was prepared by diazotization of **22** followed by cyanation. The resulting nitrile **23** was treated with TMSSnN<sub>3</sub> followed by methylation with iodomethane to afford a mixture of isomers **24a** and **24b** which are separable by chromatography. Negishi coupling of **9** or **16** with arylzincate derivatives **25a** or **25b** provided coupling products which underwent reduction to amine **6a** or **6b** (R<sub>1</sub> = 3-Me oxadiazole or *N*-2 Me tetrazole).

### Scheme 4



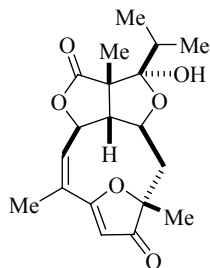
### References

- Couture, R.; Harrison, M.; Vianna, R.M.; Cloutier, F. *Eur. J. Pharmacol.* **2001**, *429*, 161–176.
- Mason, G.S.; Cumberbatch, M.J.; Hill, R.G.; Rupniak, N.M. *Can. J. Physiol. Pharmacol.* **2002**, *80*, 254–268.
- Kuduk, S.D.; Di Marco, C.N.; Chang, R.K.; Wood, M.R.; Schirripa, K.M.; Kim, J.J.; Wai, J.M.; DiPardo, R.M.; Murphy, K.L.; Ransom, R.W.; Harrell, C.M.; Reiss, D.R.; Holahan, M.A.; Cook, J.; Hess, J.F.; Sain, N.; Urban, M.O.; Tang, C.; Prueksaritanont, T.; Pettibone, D.J. and Bock, M.G. *J. Med. Chem.* **2007**, *50*, 272–282.

“Asymmetric Total Synthesis and Formal Total Synthesis of (+)-Eremantholide A”, K. J. Hale, Y. Li, *The UCL Center for Chemical Genomics, The Christopher Ingold Laboratories, The Chemistry Department, University College London, 20 Gordon Street, London WC1H 0AJ, UK.*

The presenter elaborated the total synthesis of the anti-tumor sesquiterpenoid (+)-Eremantholide A (Figure 1) which was isolated from *Eremanthus elaeagnus*, a rare woody composite that is found in Brazil. The content discussed below was obtained from a lead reference in Organic Letters (**2007**, *9*, 1267-1270).

**Figure 1**

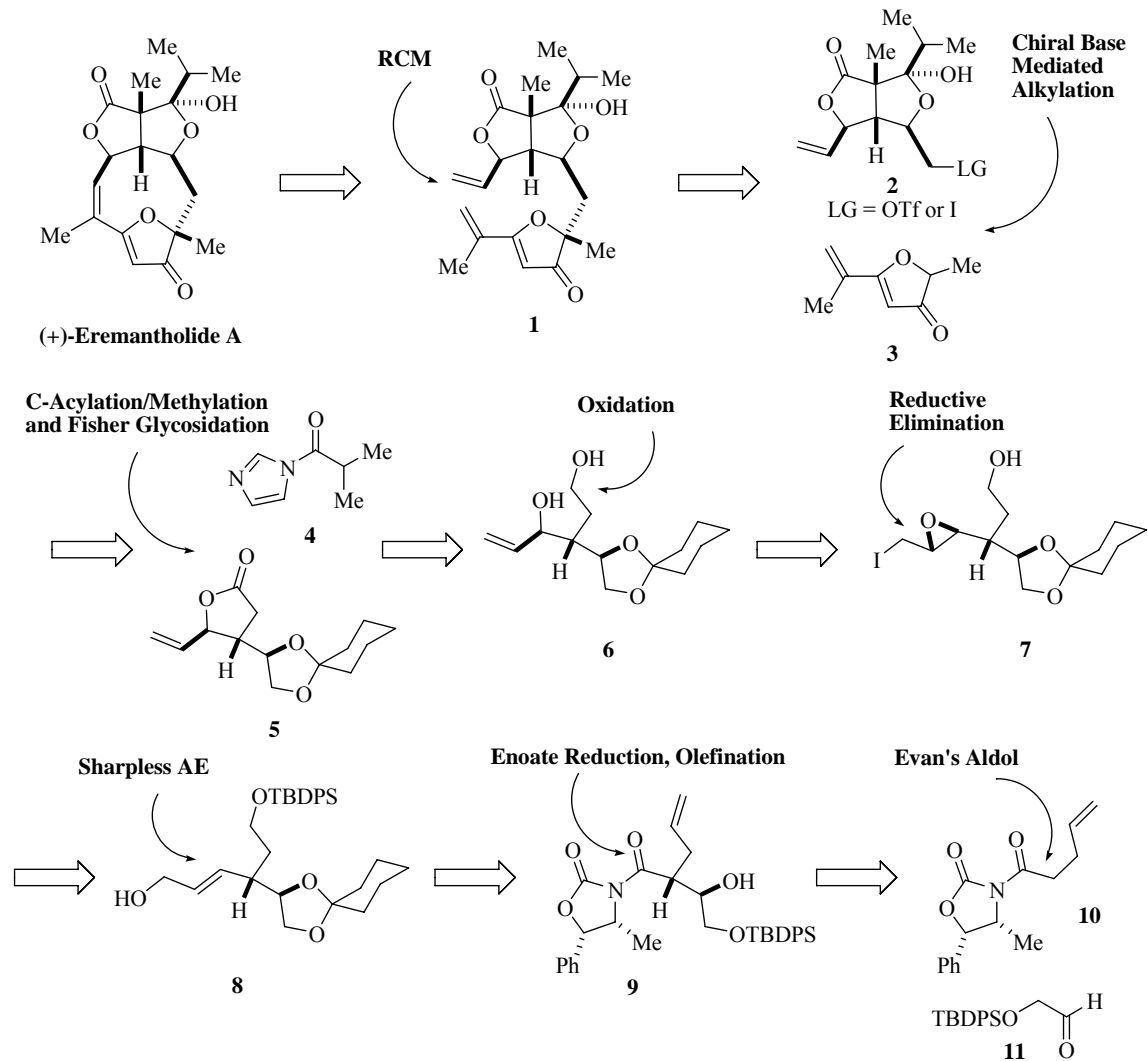


**(+)-Eremantholide A**

The target compound was discovered in 1975 by Le Quesne and Brennan and was found to have anti-tumor effects against human KB nasopharyngeal carcinoma. The mechanism of action of (+)-eremantholide A is unknown and its ability to inhibit the growth of solid tumors in the xenograft model has yet to be demonstrated. Although (+)-eremantholide A has previously been synthesized by two other research groups the researchers at University College London believe that their new asymmetric route is amenable to analogue development and will allow them to generate photoaffinity labeled probes to elucidate the mechanism of action of this molecule.

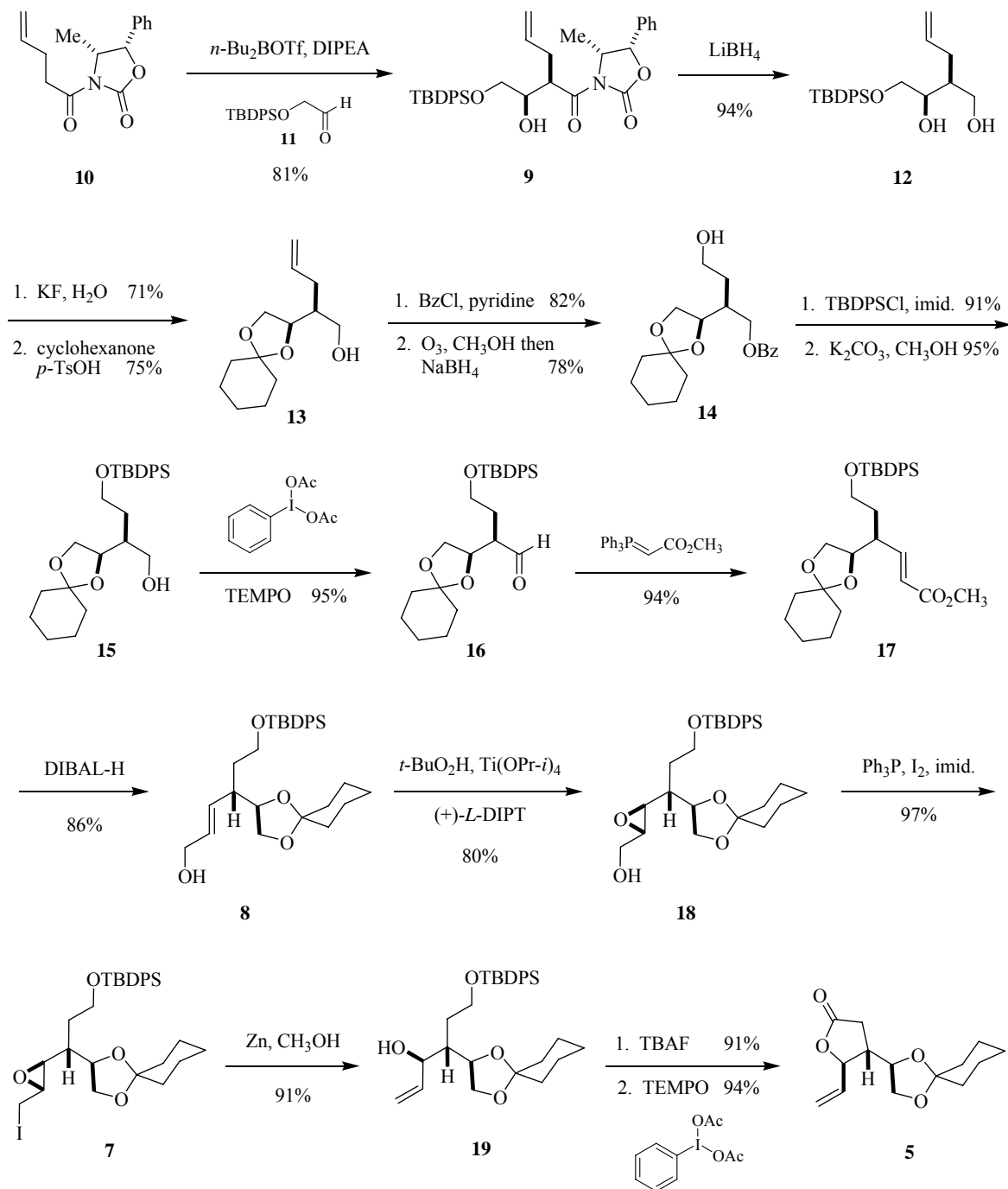
The retrosynthesis of (+)-eremantholide A is highlighted in Scheme 1. The first disconnection at the tri-substituted olefin affords the RCM precursor **1**. The quaternary center can be installed via the alkylation of the chiral enolate of intermediate **3** with **2**. The alcohol precursor to intermediate **2** would be derived from the C-acylation of **5** with **4** followed by alkylation of the resulting intermediate with methyl iodide and a Fisher glycosidation with methanol.

### Scheme 1



The butyrolactone **5** can be obtained from chemoselective oxidation of diol **6** which in turn can be obtained from the iodo-epoxide **7** by reductive elimination (Scheme 1). The epoxide is afforded by Sharpless asymmetric epoxidation of the allylic alcohol **8** followed by iodination. The C7 and C8 stereocenters in **9** can be installed using Evan's asymmetric aldol reaction between intermediates **10** and **11**.

### Scheme 2

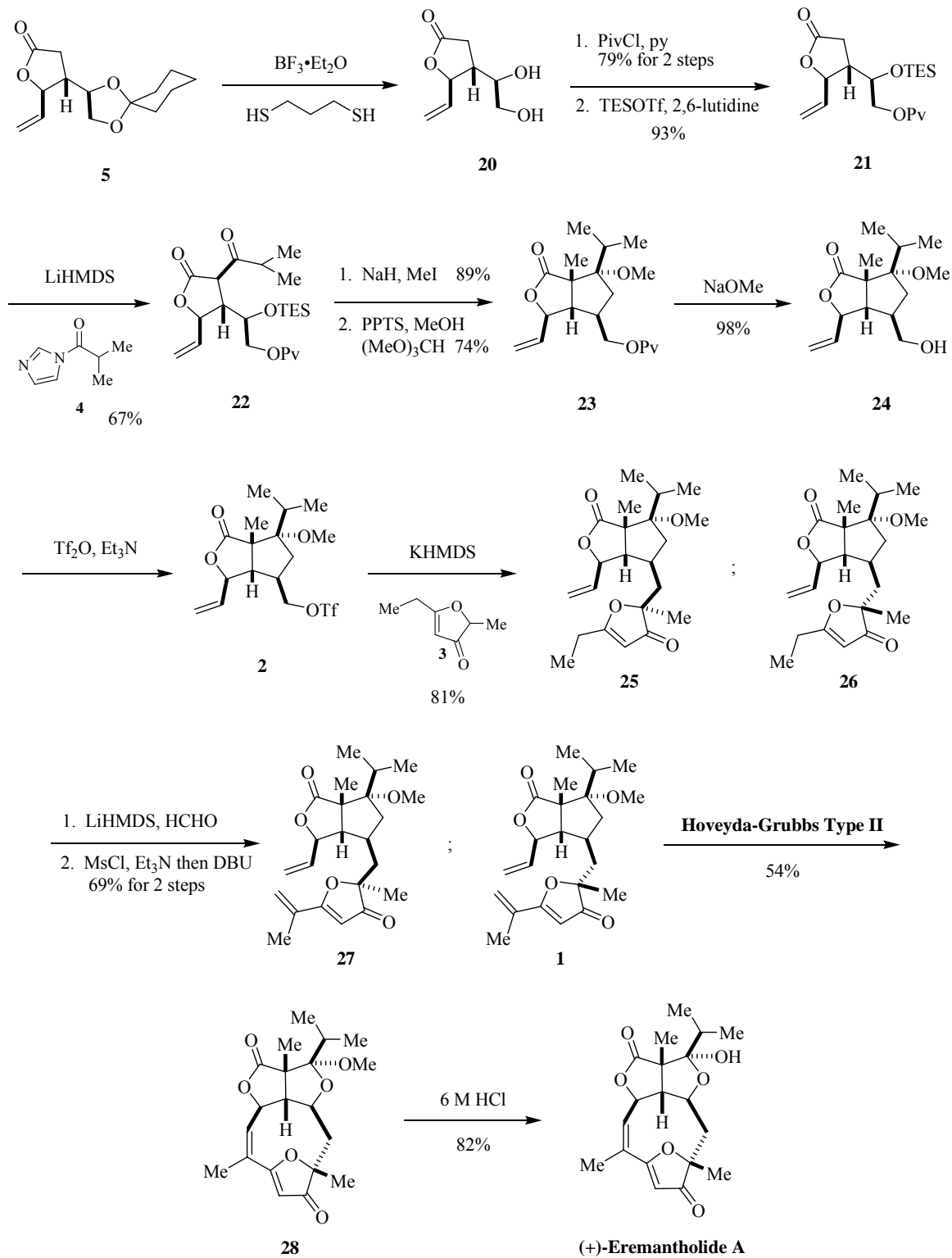


Lactone **9** was obtained by the aldol reaction of **10** and **11** to afford exclusively the desired *syn* adduct in 81% yield (Scheme 2). The chiral auxiliary was reductively removed with lithium borohydride to afford diol **12** in a 94% yield. Removal of the silyl protecting group using TBAF caused purification problems but KF was used successfully to provide the triol intermediate in 71% yield. Selective protection of the diol with cyclohexanone afforded **15** in a 75% yield without any presence of the 1,3-protected diol impurity.

Esterification of the primary alcohol with benzoyl chloride and ozonolysis of the olefin followed by a reductive workup gave alcohol **14** in 78% yield. Silylation of the primary alcohol and deprotection of the benzyl ester with potassium carbonate afforded alcohol **15** without any silyl-group migration. Oxidation of the alcohol using Swern conditions led to loss of the cyclohexylidene and TPAP/NMO conditions caused epimerization at the C7 center. Finally, conditions using TEMPO and [bis(acetoxy)iodo]benzene (BAIB) gave aldehyde **16** in 95% yield. Wittig olefination gave **17** exclusively as the *E*-isomer in 94% yield. DIBAL reduction gave alcohol **8** in 86% yield followed by Sharpless AE to give the epoxide **18** with excellent stereocontrol as a single diastereomer in 80% yield. Iodination using standard conditions was followed by reductive elimination with Zn dust to give alcohol **19** in a 91% yield. After desilylation a variety of conditions were tried to chemoselectively oxidize the diol system and after several attempts the TEMPO/BAIB conditions gave lactone **5** in excellent yields. Elaboration of the C7-position at this stage by C-acylation and C-alkylation went well but the Fisher glycosidation led to the formation of an internal acetal with the C9 oxygen. Hence, deprotection of the diol followed by selective protection of the primary and secondary alcohols gave intermediate **21** in good yields (Scheme 3). C-acylation with **4** gave the desired product in 67% yield. Alkylation of **22** with methyl iodide was followed by exposure to the Fisher glycosidation conditions cleaved the TES-group at C8 and afforded **23**. The pivaloyl group was cleaved in 98% yield and the primary alcohol was converted to the triflate **2**. The “chiral” lithium enolate of **3** was generated from lithium bis[(*S*)- $\alpha$ -methylbenzylamide] addition and alkylation gave a 2.5:1 mixture of **25/26** favoring the undesired diastereomer. Surprisingly when lithium bis[(*R*)- $\alpha$ -methylbenzylamide] was used the ration was 2.3:1 favoring the undesired diastereomer. At this stage non-chiral conditions were used to obtain **25/26** in a 1:1 ratio and the diastereomers were carried forward as a mixture at this stage. Deprotonation and quenching with formaldehyde followed by formation of the mesylate and elimination with DBU gave **27** and **1** as a mixture of products. The RCM went smoothly with **1** to afford **28** in modest 54% yield. The final step was the acid induced hydrolysis of the methyl glycoside to afford the target molecule in 82% yield.

Future work will entail the construction of novel analogues and photoaffinity labeled probes to help understand the biological mechanism of action of (+)-ermantholide A.

### Scheme 3



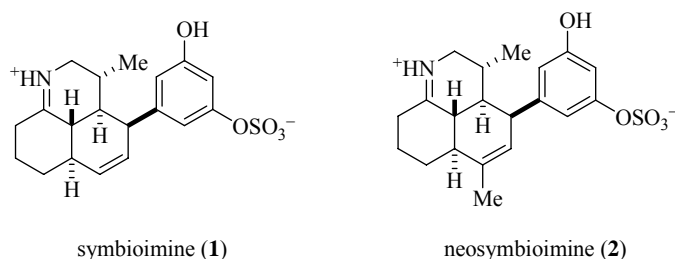
---

**“Enantioselective Total Synthesis of the Osteoclastogenesis Inhibitor (+)-Symbioimine”, J. Kim and Regan J. Thomson, Department of Chemistry, Northwestern University, 2145 Sheridan Rd., Evanston, IL 60208 and Department of Chemistry and Chemical Biology, Harvard University 12 Oxford St., Cambridge, MA 02138.**

This presentation discussed the enantioselective total synthesis of (+)-symbioimine which is an unusual tetracyclic alkaloid that was isolated from *Symbiodinium* sp. The content discussed below was obtained from a lead reference in *Angewandte Chemie* (2007, 46, 1-4).

The target molecule (Figure 1) inhibits osteoclastogenesis in RAW264 cells ( $EC_{50} = 44 \mu\text{g/mL}$ ). Symbioimine was also found to inhibit cyclooxygenase-2 activity suggesting that it may have a potential use as an anti-inflammatory agent. The closely related compound Neosymbioimine was reported in 2005.

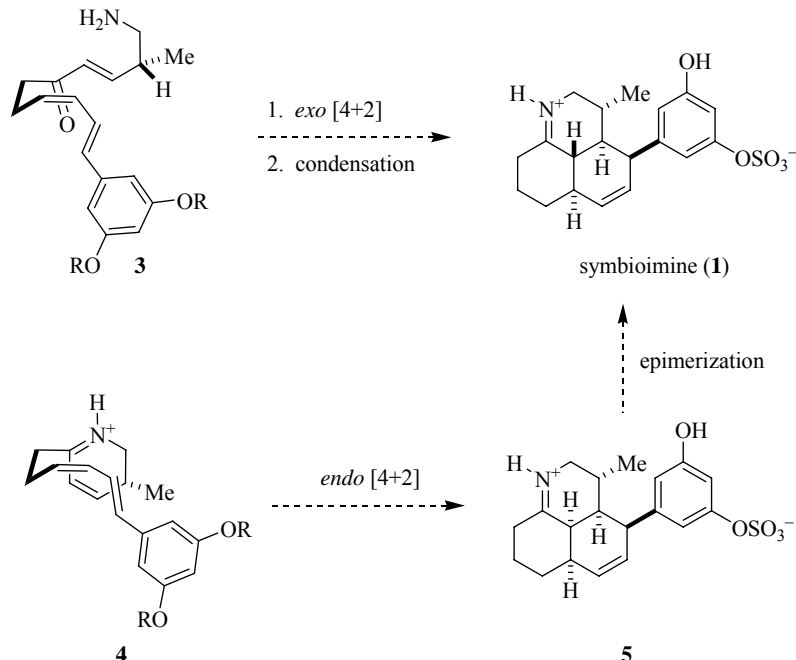
**Figure 1**



The Uemura group isolated and elucidated the structure and biological activity of symbioimine and proposed that the biosynthesis of **1** may arise from the *exo*-selective Diels-Alder reaction on intermediate **3** (Scheme 1). However, Kim and Thomson believed that it would require the presence of an enzyme to proceed *exo* selectively and they proposed an *endo*-selective cyclization of the iminium ion **4** (Scheme 1). Hence diastereomer **5** would arise from an addition opposite to the methyl group. Epimerization of the *cis*-fused system should afford the thermodynamically favored *trans*-fused ring system to afford **1**. While Kim and Thomson were investigating their hypothesis, Uemura and co-workers published a similar idea and Snider and Che reported a model study that successfully completed the Diels-Alder reaction followed by epimerization. To date two total syntheses of **1** have been reported however the one discussed below is the first enantioselective total synthesis of (+)-symbioimine.

Aldehyde **6** underwent a Horner-Wadsworth-Emmons reaction to afford the diene **7** in 82% yield with >11:1 *E:Z* selectivity (Scheme 2). The methyl ketone **8** was obtained in 90% yield by formation of the Weinreb amide followed by nucleophilic attack with MeMgCl. The silyl enol ether **9** was formed in 70% yield using Corey's protocol. Reaction of **9** with the dimethyl acetal **10** in the presence of TMSOTf gave adduct **11** in 58% yield. Treatment with sodium azide followed by a Staudinger reaction gave the imine **12** in a 98% yield for the two steps.

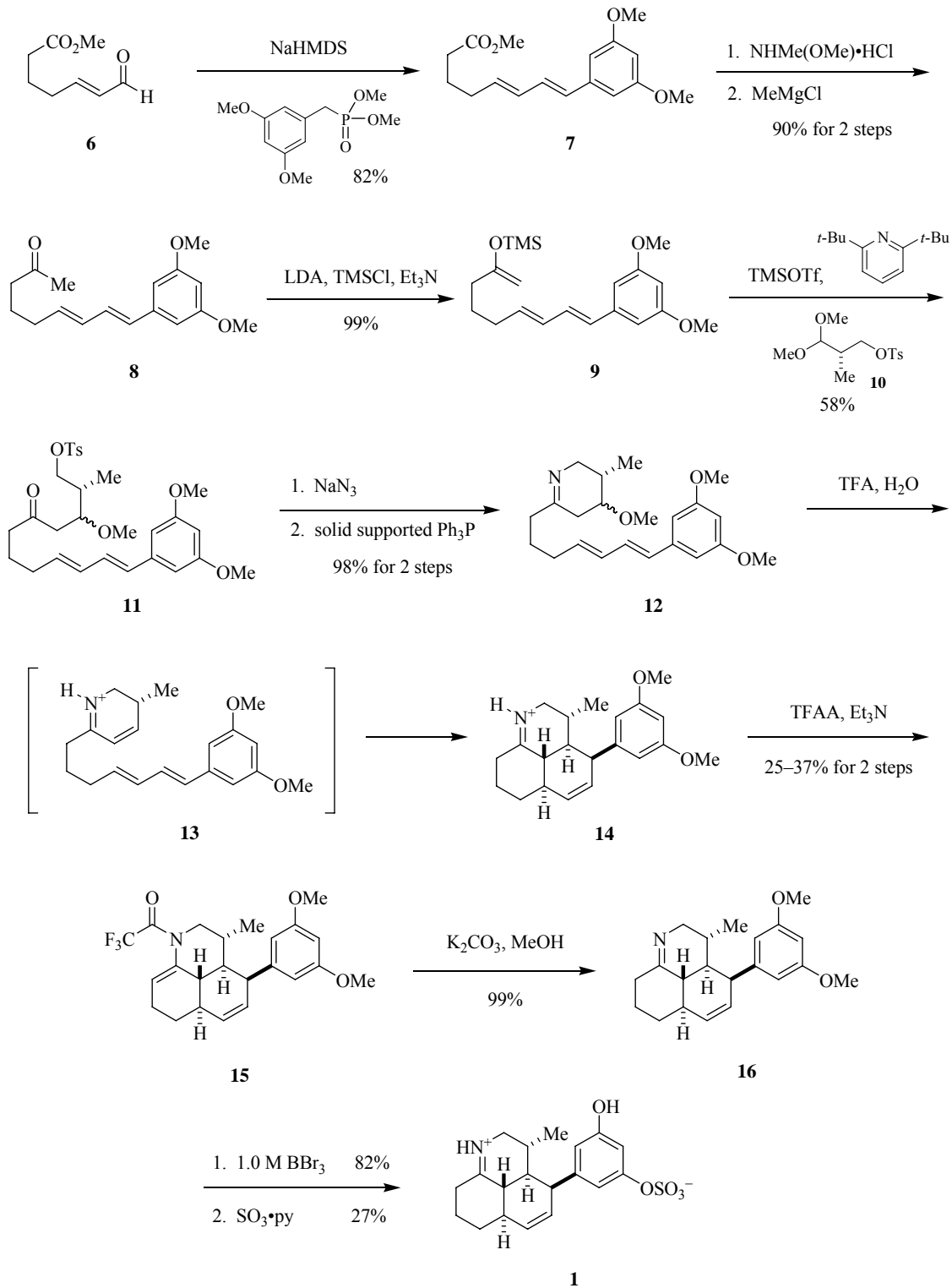
### Scheme 1



Thermal elimination of methanol from **12** led to decomposition products. However, heating **12** in the presence of aqueous TFA afforded the cycloadduct **14** presumably by the pathway shown in Scheme 2. Elimination of methanol under the acidic conditions forms the intermediate dihydropyridine **13** which undergoes a Diels-Alder reaction (*endo* [4+2]). The proton NMR of **14** indicated that there was only one diastereomer present in the reaction mixture. For ease of purification the reaction mixture was treated with TFAA to afford **15** in a 25-37% yield for the two steps. At this stage some NOE studies helped confirm the structure of the tricyclic ring system. Under basic conditions the trifluoroacetate moiety was cleaved to obtain **16** in a 99% yield. Removal of the methyl ethers in 82% yield was followed by sulfation using conditions reported by Maier and co-workers to provide **1** in 27% yield. The optical rotation and spectroscopic data of **1** corresponded with the literature data.

The authors highlighted the fact that their Diels-Alder reaction is unique in that it proceeds via iminium ion intermediates as opposed to acyl iminium or ketone intermediates. The moderate yields might be associated with pyridine containing by-products however no unusual structures such as the ones reported by Snider and co-workers were isolated. The concise nature of this synthesis allows for analogue synthesis and more importantly structure-activity relationship studies.

## Scheme 2



---

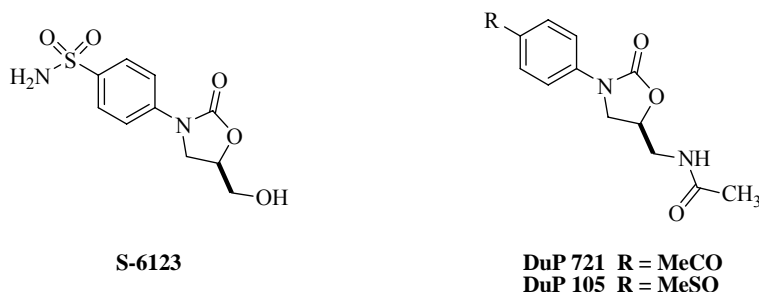
**“Zyvox® the first member of a completely new class of antibacterial agents for treatment of serious gram-positive infections”, S. J. Brickner, M.R. Barbachyn, D. K. Hutchinson and P. R. Manninen.**

The researchers were given the ACS award for team innovation. The content discussed below was obtained from a lead reference in the Journal of Medicinal Chemistry (1996, 39, 673-679).

Zyvox® was developed to provide humans with a way to combat serious Gram-positive bacterial infections. This discovery was particularly timely since vancomycin-resistant enterococcal (VRE) isolates were found in both the U.S and U.K.

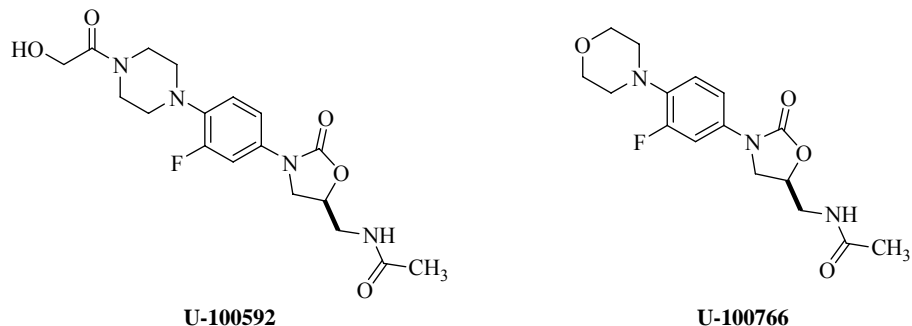
A patent issued by EI DuPont de Nemours & Co. in 1978 contained a series of 5-(halomethyl)-3-aryl-2-oxazolidinones that claimed to have activity against certain plant pathogens. Eventually S-6123 (Figure 1) was described as having weak *in vivo* antibacterial activity against human pathogens. This compound was further developed into two drug candidates, DuP 721 and DuP 105 (Figure 1) which were known as a new class of orally active and completely synthetic antibacterial agents. The mode of action of these compounds was inhibition of bacterial protein synthesis. Both compounds were entered into phase I but their development was discontinued. Research done at Upjohn Co. showed that DuP 721 caused lethal toxicity in the rat at 100 mg/kg b.i.d. for thirty days.

**Figure 1**



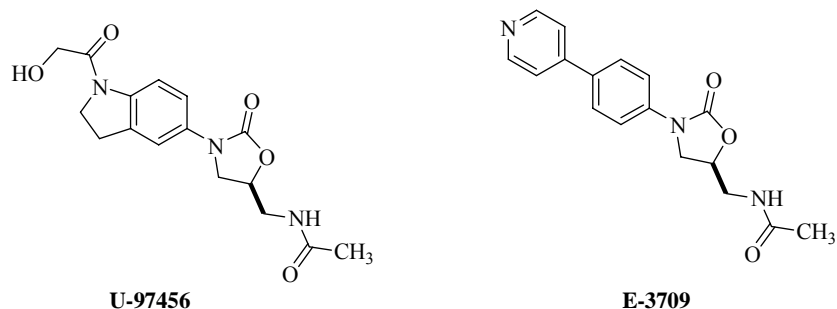
Researchers at Upjohn decided to pursue the oxazolidinones in attempts to improve the biological profile of DuP 721 and toward this end the novel oxazolidinones U-100592 and U-100766 (Zyvox®, linezolid) were developed (Figure 2).

**Figure 2**



Both compounds, U-97456 (Upjohn) and E-3709 (DuPont) are known potent compounds. Based on the location of the indolinyl nitrogen in U-97456 and the pyridyl nitrogen in E-3709 it was considered worthwhile to explore a piperazine in that part of the molecule and it was found that a hydroxyacetyl moiety on the terminus helped maintain antibacterial activity. Furthermore, the incorporation of a fluorine atom on the phenyl ring enhanced *in vitro* and *in vivo* potency of U-100592. After extensive SAR development the incorporation of morpholine, a bioisostere of piperazine, led to the discovery of linezolid.

**Figure 3**



The synthesis of both U-100592 and U-100766 is described in Scheme 1. Nucleophilic displacement of the *p*-fluoro by either piperazine or morpholine afforded **3a-b** in good yields. Reduction of the nitro group gave anilines **4a-b** which were protected with CBz-Cl to afford intermediates **5a-b**. The key oxazolidinone forming step was carried out by generating the lithium anion of **5a-b** followed by addition of (*R*)-glycidyl butyrate. The resulting primary alcohols **6a-b** were converted to the mesylates **7a-b** and displaced with potassium phthalimide in the case of **7a** and sodium azide in the case of **7b**. Intermediate **8a** was treated with dimethylamine and intermediate **8b** was hydrogenated to afford the primary amines **9a-b** that were acylated to afford compounds **10** and **11** (U-100766, Zyvox®). Intermediate **10** was further manipulated as shown in Scheme 1 to obtain **14** (U-100592). Both these compounds had potency levels similar to that of vancomycin and neither of them showed efficacy toward Gram-negative strains. Finally, excellent activity was seen against vancomycin-resistant *E. faecium* in the lethal systemic mouse model.

### Scheme 1

